AD_____

Award Number: W81XWH-08-1-0042

TITLE: PTEN Loss Antagonizes Calcitriol-mediated Growth Inhibition in Prostate Epithelial Cells

PRINCIPAL INVESTIGATOR: Linara S. Axanova, M.S.

CONTRACTING ORGANIZATION: Wake Forest University Health Sciences

Winston Salem, North Carolina
27157-0001

REPORT DATE: May 2010

TYPE OF REPORT: Annual Summary

PREPARED FOR: U.S. Army Medical Research and Materiel Command
Fort Detrick, Maryland 21702-5012

DISTRIBUTION STATEMENT:

X Approved for public release; distribution unlimited

The views, opinions and/or findings contained in this report are those of the author(s) and should not be construed as an official Department of the Army position, policy or decision unless so designated by other documentation.

REPORT DOCUMENTATION PAGE

Form Approved
OMB No. 0704-0188

Public reporting burden for this collection of information is estimated to average 1 hour per response, including the time for reviewing instructions, searching existing data sources, gathering and maintaining the data needed, and completing and reviewing this collection of information. Send comments regarding this burden estimate or any other aspect of this collection of information, including suggestions for reducing this burden to Department of Defense, Washington Headquarters Services, Directorate for Information Operations and Reports (0704-0188), 1215 Jefferson Davis Highway, Suite 1204, Arlington, VA 22202-4302. Respondents should be aware that notwithstanding any other provision of law, no person shall be subject to any penalty for failing to comply with a collection of information if it does not display a currently valid OMB control number. **PLEASE DO NOT RETURN YOUR FORM TO THE ABOVE ADDRESS.**

1. REPORT DATE *(DD-MM-YYYY)*
01-05-2010

2. REPORT TYPE
Annual

3. DATES COVERED *(From - To)*
April 21, 2009 – April 20, 2010

4. TITLE AND SUBTITLE

PTEN Loss Antagonizes Calcitriol-mediated Growth Inhibition in Prostate Epithelial Cells

5a. CONTRACT NUMBER

5b. GRANT NUMBER
W81XWH-08-1-0042

5c. PROGRAM ELEMENT NUMBER

6. AUTHOR(S)
Linara S. Axanova

5d. PROJECT NUMBER

5e. TASK NUMBER

5f. WORK UNIT NUMBER

7. PERFORMING ORGANIZATION NAME(S) AND ADDRESS(ES)
Wake Forest University Health Sciences
Winston Salem, North Carolina
27157-0001

8. PERFORMING ORGANIZATION REPORT NUMBER

9. SPONSORING / MONITORING AGENCY NAME(S) AND ADDRESS(ES)
U.S. Army Medical Research
and Material Command
Fort Detrick, Maryland
21702-5012

10. SPONSOR/MONITOR'S ACRONYM(S)

11. SPONSOR/MONITOR'S REPORT NUMBER(S)

12. DISTRIBUTION / AVAILABILITY STATEMENT

Approved for public release; distribution unlimited

13. SUPPLEMENTARY NOTES

14. ABSTRACT

BACKGOUND: 1-alpha, 25-dihydroxy vitamin D_3 ($1,25(OH)_2D_3$) inhibits proliferation of multiple cancer cell types including prostate cells and upregulates p21 and/or p27, while loss of Pten and PI3K/AKT activation stimulates survival and downregulates p21 and p27. We hypothesized that inhibition of the PI3K/AKT pathway synergizes with the antiproliferative signaling of $1,25(OH)_2D_3$. METHODS: Viability, cell cycle and senescence of cells were evaluated upon combinational treatment with $1,25(OH)_2D_3$ and pharmacological PI3K/AKT inhibitors**.** RESULTS: Pharmacological inhibitors of PI3K or Akt and $1,25(OH)_2D_3$ synergistically inhibited growth of DU145, LNCaP, primary human prostate cancer cell strains and Pten null mouse prostatic epithelial cells (MPEC). The inhibitors used included API-2 (Triciribine) and GSK690693 which are currently in clinical trials for treatment of cancer. A novel mechanism for antiproliferative effects of $1,25(OH)_2D_3$ in prostate cells, induction of senescence, was discovered. Combination of $1,25(OH)_2D_3$ and AKT inhibitor cooperated to induce G_1 arrest, senescence, and p21 levels in prostate cancer cells. As AKT is commonly activated by PTEN loss, we evaluated the role of Pten in responsiveness to $1,25(OH)_2D_3$ using shRNA knockdown and by *in vitro* knockout of Pten. MPEC that lost Pten expression remained sensitive to the antiproliferative action of $1,25(OH)_2D_3$, and showed higher degree of synergism between AKT inhibitor and $1,25(OH)_2D_3$ compared to Pten-expressing counterparts. CONCLUSIONS: These findings provide the rationale for the development of therapies utilizing $1,25(OH)_2D_3$ or its analogs combined with inhibition of PI3K/AKT for the treatment of prostate cancer.

15. SUBJECT TERMS
Vitamin D_3, AKT inhibition, synergism, prostate cancer

16. SECURITY CLASSIFICATION OF:			**17. LIMITATION OF ABSTRACT**	**18. NUMBER OF PAGES**	**19a. NAME OF RESPONSIBLE PERSON**
a. REPORT	**b. ABSTRACT**	**c. THIS PAGE**			**19b. TELEPHONE NUMBER** *(include area code)*
U	U	U	UU	47	

Standard Form 298 (Rev. 8-98)
Prescribed by ANSI Std. Z39.18

Table of Contents

	Page
Introduction……..…..	**4**
Body……..	**6**
Key Research Accomplishments……..	**13**
Reportable Outcomes……	**13**
Conclusion……	**14**
References……	**15**
Appendices……	**17**
Article published in Prostate Journal (in press)……..	**17**

Introduction

Prostate cancer (CaP) is the most commonly diagnosed cancer and the second most common cause of cancer death in American men [1]. It has been suggested that the development of clinical prostate cancer may be associated with vitamin D_3 deficiency [2, 3].

Vitamin D is a hormone that can be obtained from the diet or produced endogenously by a series of reactions that culminates in the most active metabolite of vitamin D, 1α, 25$(OH)_2$-vitamin D_3 (1,25$(OH)_2D_3$). The classical targets of 1,25$(OH)_2D_3$ are kidney, intestine and bone where it maintains serum calcium levels within narrow range required for several vital functions such as bone mineralization, immune and neuromuscular function, signal transduction and blood coagulation [4]. Hormonally active 1,25$(OH)_2D_3$ is synthesized from vitamin D_3 (also called cholecalciferol). Vitamin D_3 can be obtained from dietary sources such as milk and fish oils or can be synthesized endogenously. During endogenous synthesis, UVB rays provide the energy required to convert 7-dehydrocholesterol present in the skin to vitamin D_3. Vitamin D_3 from the skin is first transported to the liver. In the liver, a mitochondrial enzyme 25-hydroxylase hydroxylates the C25 position of vitamin D_3 to generate 25$(OH)D_3$ [5]. 25$(OH)D_3$ is then transported to kidney where hydroxylation at the C1 position by an enzyme 1α-hydroxylase results in the hormonally active form of vitamin D_3, 1,25$(OH)_2D_3$ [6]. Normal circulating levels of 1,25$(OH)_2D_3$ in plasma is in the pico mole range and is ~a 1000 fold lower than that of 25$(OH)D_3$. The half life of 1,25$(OH)_2D_3$ in circulation was determined to be between 4 and 6 hours [7] while the half life of 25$(OH)D_3$ is about 30 days [8]. 1,25$(OH)_2D_3$ regulates its synthesis by inhibiting the production of renal 1α-hydroxylase, as well as by inducing expression of an enzyme which initiates degradation and excretion of 1,25$(OH)_2D_3$. The mechanism of synthesis and degradation of 1,25$(OH)_2D_3$ is tightly regulated in order to maintain serum calcium levels within normal range. Abnormal increase in 1,25$(OH)_2D_3$ may result in hypercalcemia which on its turn may cause a variety of symptoms ranging from dehydration and kidney stones to coma and death.

1,25$(OH)_2D_3$ elicits antiproliferative effects in a variety of cancer cell types including cell lines derived from prostate [9, 10]. The ability of 1,25$(OH)_2D_3$ to inhibit prostate growth was also demonstrated in primary prostatic cells from histologically normal, benign prostatic hyperplasia (BPH), and prostate cancer specimens [11], in multiple prostate cancer cell lines [12-14], in xenograft models of prostate cancer [15, 16] as well as in Dunning rat prostate model [17]. The anticancer mechanisms of 1,25$(OH)_2D_3$'s action include induction of cell cycle arrest, promotion of differentiation, inhibition of proliferation and angiogenesis, as well as inhibition of invasive and migratory potential of cancer cells [reviewed in [18]].

Classical actions of 1,25$(OH)_2D_3$ are mediated through the vitamin D receptor (VDR) which is a member of a superfamily of nuclear steroid hormone receptors. Upon 1,25$(OH)_2D_3$ binding VDR

translocates to the nucleus, dimerizes with retinoid X receptor (RXR) and modulates the expression of target genes. Although a number of 1,25$(OH)_2D_3$ responsive genes are known, the exact mechanism of growth regulation by 1,25$(OH)_2D_3$ is not completely defined; however, an increase in p21 and/or p27 is an almost universal feature [9].

One of the central contributing factors which facilitates the survival of prostate cancer cells is attributed to the phosphoinositol-3 kinase PI3K-AKT pathway. Activated AKT phosphorylates a host of proteins that affect cell growth, cell cycle entry, and cell survival. The AKT pathway presents an attractive target for anticancer therapies and several AKT inhibitors have been developed that demonstrate anticancer activity in preclinical and clinical studies [19]. In prostate cancer, activation of AKT occurs most frequently due to the loss of tumor suppressor phosphatase and a tensin homologue deleted in chromosome ten (PTEN)[20-22]. Loss of PTEN protein occurs in 20% of primary prostate tumors and this loss is highly correlated with advanced tumor grade and stage with 50% of metastatic tumors exhibiting a loss of PTEN protein [23]. Moreover, loss of heterozygosity (LOH) is found in 20% to 60% of metastatic tumors [24]. Data suggests that advancing disease is associated with a progressive loss of PTEN or an accumulation of mutations in the PTEN gene. Loss of PTEN and activation of AKT has been shown to downregulate the expression of p21 and p27 by a number of mechanisms [25-30].

In our preliminary data we had shown that *Pten* WT mouse prostatic epithelial cells (MPEC) exhibit significant levels of growth-inhibition in response to the presence of 1,25$(OH)_2D_3$, whereas growth of *Pten*-/- MPECs in which Pten was lost *in vivo* are not affected by 1,25$(OH)_2D_3$. Pretreatment of *Pten*-/- MPECs with PI3K/AKT inhibitors resulted in the partial restoration of sensitivity to 1,25$(OH)_2D_3$. Given our preliminary findings and the existing data contained within recent literature, we proposed the hypothesis that **1,25$(OH)_2D_3$-mediated growth inhibition of prostate epithelial cells is antagonized by PTEN loss**.

Body

As it was described in the previous (2008-2009) Annual Report we evaluated the role of Pten in responsiveness to $1,25(OH)_2D_3$ using shRNA knockdown and by *in vitro* knockout of Pten. We demonstrated that MPEC that lost Pten expression remained sensitive to the antiproliferative action of $1,25(OH)_2D_3$. These data demonstrate that while *in vivo* loss of Pten was associated with resistance to $1,25(OH)_2D_3$-mediated growth inhibition of MPEC as demonstrated by our preliminary data, *in vitro* suppression or loss of Pten in MPECs was not associated with increased resistance to $1,25(OH)_2D_3$. Thus our initial hypothesis that Pten loss antagonizes $1,25(OH)_2D_3$-mediated growth inhibition of prostate epithelial cells was not confirmed.

Interestingly, we found that pharmacological inhibitors of PI3K or Akt and $1,25(OH)_2D_3$ synergistically inhibited growth of DU145, LNCaP, primary human prostate cancer cell strains and Pten null mouse prostatic epithelial cells (MPEC). The inhibitors used included API-2 (Triciribine) and GSK690693 which are currently in clinical trials for treatment of cancer. A novel mechanism for antiproliferative effects of $1,25(OH)_2D_3$ in prostate cells, induction of senescence, was discovered. Combination of $1,25(OH)_2D_3$ and AKT inhibitor cooperated to induce G_1 arrest and senescence. These findings provided the rationale for prostate cancer therapies involving use of AKT inhibitors and $1,25(OH)_2D_3$ in adjunctive therapy.

2009-2010 Progress

Part I. In 2009-2010 we further developed the study described in the 2008-2009 Annual Report. The results are summarized in a manuscript that is now accepted for publication in Prostate and currently is in press (the manuscript is attached).

In brief, we sought to evaluate the effect of AKT inhibition and $1,25(OH)_2D_3$ treatment on protein levels of $p21^{Cip1}$ and $p27^{Kip1}$role since the antiproliferative effects of $1,25(OH)_2D_3$ are known to commonly involve upregulation of $p21^{Cip1}$ and/or $p27^{Kip1}$. Our results demonstrated that treatment with API-2 and $1,25(OH)_2D_3$ cooperated to increase $p21^{Cip1}$ protein (Fig. 3F of the attached manuscript). These data suggest that synergism between API-2 and $1,25(OH)_2D_3$ in prostate cancer cells might be a result of cooperative induction of cell cycle arrest and senescence possibly through induction of $p21^{Cip1}$ levels.

We also evaluated the effect of Pten status on the presence of synergism between $1,25(OH)_2D_3$ and AKT inhibitor API-2. WFU3 Control shRNA MPEC (the clone with the lowest levels of phosphor-

Ser473 Akt) and WFU3 Pten shRNA MPEC (the clone with the highest levels of phospho- Ser473 Akt and phosphor-Thr308 Akt) were treated with 1,25$(OH)_2D_3$, API-2 or with multiple combinations of the two compounds. Out of all dose combinations tested the control clone MPEC showed "intermediate" synergism at 10nM 1,25$(OH)_2D_3$ combined with 50nM or 100nM API-2 (Fig.5A, Table III of the attached manuscript). On the other hand, MPEC with Pten knock down showed "*very strong"* to *"strong"* synergism throughout all tested dose combinations of 1,25$(OH)_2D_3$ and API-2 as determined by the CI values (Fig. 5B, Table III of the attached manuscript). A similar trend was observed in the MPEC with Pten deleted using Cre-recombinase. Briefly, $Pten^{lox/lox}$ MPEC demonstrated only "intermediate" synergism between 1,25$(OH)_2D_3$ and API-2 at 10nM 1,25$(OH)_2D_3$ combined with 5nM and 50nM API-2, while the $Pten^{-/-}$ MPEC demonstrated "strong" to "very strong" synergism at the highest dose of API-2 tested (500nM) combined with any dose of 1,25$(OH)_2D_3$ (data not shown).

Together, data demonstrated that suppression or loss of Pten in MPECs was not associated with increased resistance to growth-inhibitory qualities of 1,25$(OH)_2D_3$ in MPEC. In addition, our data suggests that loss of Pten might strengthen the synergistic effect between 1,25$(OH)_2D_3$ and AKT inhibition on cellular growth inhibition.

In conclusion, these findings provide the rationale for the development of therapies utilizing 1,25$(OH)_2D_3$ or its analogs combined with inhibition of PI3K/AKT for the treatment of prostate cancer.

<u>Part II:</u> Growth inhibition of prostate cancer cells by 1,25$(OH)_2D_3$: role of senescence.

The mechanism of growth inhibition mediated by 1,25$(OH)_2D_3$ in prostate cells is not completely elucidated. Our finding showed that 1,25$(OH)_2D_3$ was able to induce senescence in prostate cells. The ability of 1,25$(OH)_2D_3$ to induce senescence has *not* been demonstrated before and contributes to the understanding of the antiproliferative effects of 1,25$(OH)_2D_3$ in prostate cells. Thus, we further evaluate the ability of 1,25$(OH)_2D_3$ to induce senescence in prostate cells as well as study mechanism of this induction.

Senescent cells are described as a cell permanently arrested in the cell cycle. These cells are refractory to proliferation stimuli, exhibit altered cell morphology and gene expression while remaining viable and preserving metabolic activity (reviewed in [31]). There are multiple data demonstrating that senescence is a mechanism that limits cellular lifespan and presents a barrier for cellular immortalization and progression of tumorigenesis [32, 33]. DNA damage or oncogene expression can induce cellular senescence and in order to become immortal cells have to overcome senescence by acquiring additional genetic alterations.

A process of senescence was demonstrated to have a significant role in human cancers as well. It was shown that human benign tumors contain senescent cells and that these cells disappear in their malignant counterparts [34, 35]. In human prostate cancer Majumder et al. [36] demonstrated that markers of cellular senescence are elevated in PIN when compared to nondysplastic elithelial cells in the same tissue section. Chen et al. [37] showed that in specimens from early-stage human prostate cancer markers of senescence were present in areas of prostate hyperplasia/PIN and rarely in areas of carcinoma. These findings suggest a role for senescence as a barrier for progression of tumorigenesis in prostatic cells. The ability of $1,25(OH)_2D_3$ to induce senescence in human primary prostate cancer cell strain demonstrated in the study supports utilization of $1,25(OH)_2D_3$ for the treatment of earlier stages of human prostate cancer with the goal of prevention of disease progression.

In spite of strong proliferative effects on prostatic cells, treatment of prostate cancer with $1,25(OH)_2D_3$ is limited due to the calcium mobilizing effects of high dose $1,25(OH)_2D_3$ [38,39]. In 1998, Schwartz et al. showed that human primary prostatic epithelial cells (HPEC) express 1α-hydroxylase and can convert 25(OH)D3 to $1,25(OH)_2D_3$ [40]. In addition, we have previously observed that $25(OH)D_3$ induced strong antiproliferative effects in HPEC (unpublished data). Moreover, recent data demonstrated that prostate cells express 25(OH)-hydroxylase [41] suggesting that $1,25(OH)_2D_3$ can be synthesized in prostate cells in autocrine manner from cholecalciferol (cholecalciferol to $25(OH)D_3$ to $1,25(OH)_2D_3$). Thus, in addition to testing role of $1,25(OH)_2D_3$ on induction of senescence in prostate cells, we are also interested in testing the ability of cholecalciferol and $25(OH)D_3$ to induce senescence in human prostatic epithelial cells.

We have isolated normal, BPH as well as cancer human primary cell strains as previously described [42]. Two cell strains of normal, BPH, and cancer human primary cells are used in the experiments. We are assessing growth inhibition (by trypan blue viability assay) and senescence (β-galactosidase activity) upon treatment with increasing doses of $1,25(OH)_2D_3$, $25(OH)D_3$ and cholecalciferol. We also isolate RNA and proteins at various time points upon treatment.

Our preliminary data is demonstrated below in the Figures P-1 through P-4. We observed that 27% of the WFU55 (normal human prostate epithelial cell strain) cells were undergoing senescence after treatment with 100 nM $1,25(OH)_2D_3$ (Figure P-1). The results obtained using other cell strains as well as results from experiments utilizing cholecalciferol and $25(OH)D_3$ are being analyzed.

In addition to human primary cell strains we confirmed ability of $1,25(OH)_2D_3$ to induce senescence in mouse prostatic progenitor cells that have been isolated in our lab [43]. Over 40% of the WFU3 clone 3 prostatic progenitor MPEC were positive for the senescence-associated β-galactosidase activity (Figure P-2).

We further sought to evaluate the role of Pten in the ability of $1,25(OH)_2D_3$ to induce senescence. Thus, we treated Pten flox/flox MPEC as well as Pten-/- MPEC with increasing concentrations of $1,25(OH)_2D_3$ and assessed induction of senescence by senescence-associated β-galactosidase activity. Our preliminary data suggests presence of more pronounced senescence in cells that have lost Pten expression as well as increased ability of $1,25(OH)_2D_3$ to induce senescence in the cells lacking Pten. Quantification of this data is in progress (Figure P-3). Similar results were observed in MPEC where Pten was knocked down using shRNA approached (as described in the Materials and Methods section of the attached manuscript) (Figure P-4).

Next, we would like to evaluate the role of p21 and p27 in the induction of senescence in prostate cells by $1,25(OH)_2D_3$. To do so, we designed shRNA sequences and have generated a lentivirus that we will use to infect the human primary prostate epithelial cells. We hypothesize that p21 and/or p27 is critical for the induction of senescence in prostatic cells.

Figure P-1: Growth inhibition and induction on senescence in human primary prostate epithelial cell strain WFU55 upon treatment with increasing concentration of $1,25(OH)_2D_3$.

P-1A. Representative photographs of senescence induction in WFU55 human primary epithelial prostate cells treated with increasing concentrations of $1,25(OH)_2D_3$ as determined by senescence-associated β-galactosidase activity. Cells treated with Doxorubicin were used as a positive control. For negative control senescence was assessed at pH 7 in Doxorubicin-treated cells.

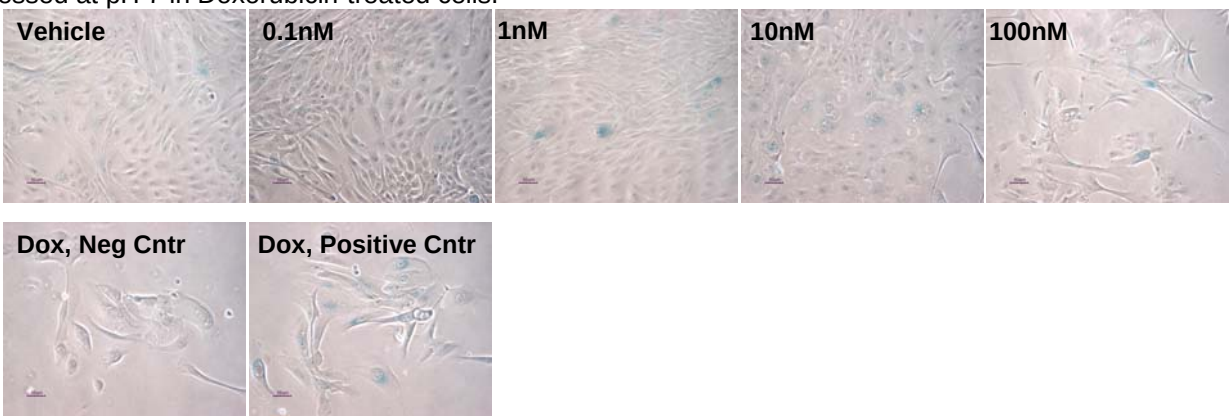

P-1B. Growth inhibition of WFU55 human primary epithelial prostate cell strain treated with increasing concentration of $1,25(OH)_2D_3$ as determined by trypan blue viability assay.

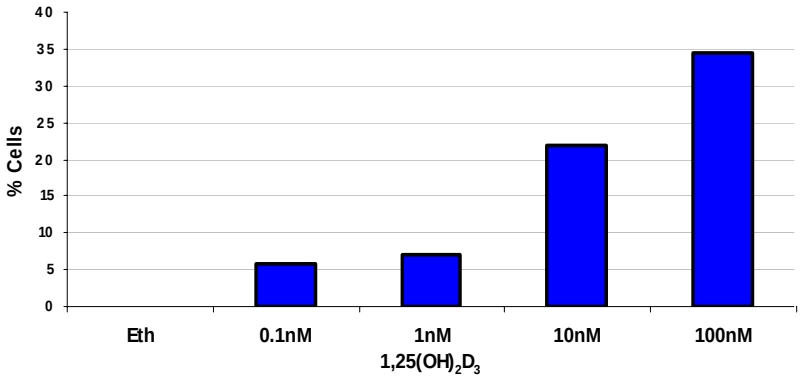

P-1C. Quantification of senescence evaluation of WFU55 human primary epithelial prostate cells treated with increasing concentrations of $1,25(OH)_2D_3$ as determined by senescence-associated β-galactosidase activity.

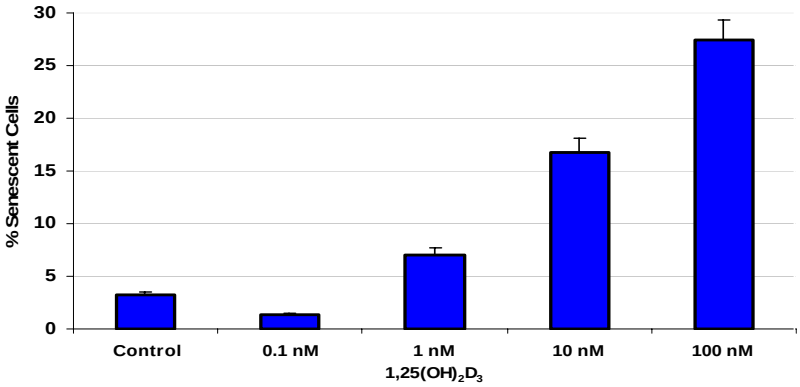

Figure P-2. Induction of senescence in WFU3 clone 3 mouse prostatic epithelial cells as determined by senescence-associated β-galactosidase activity.

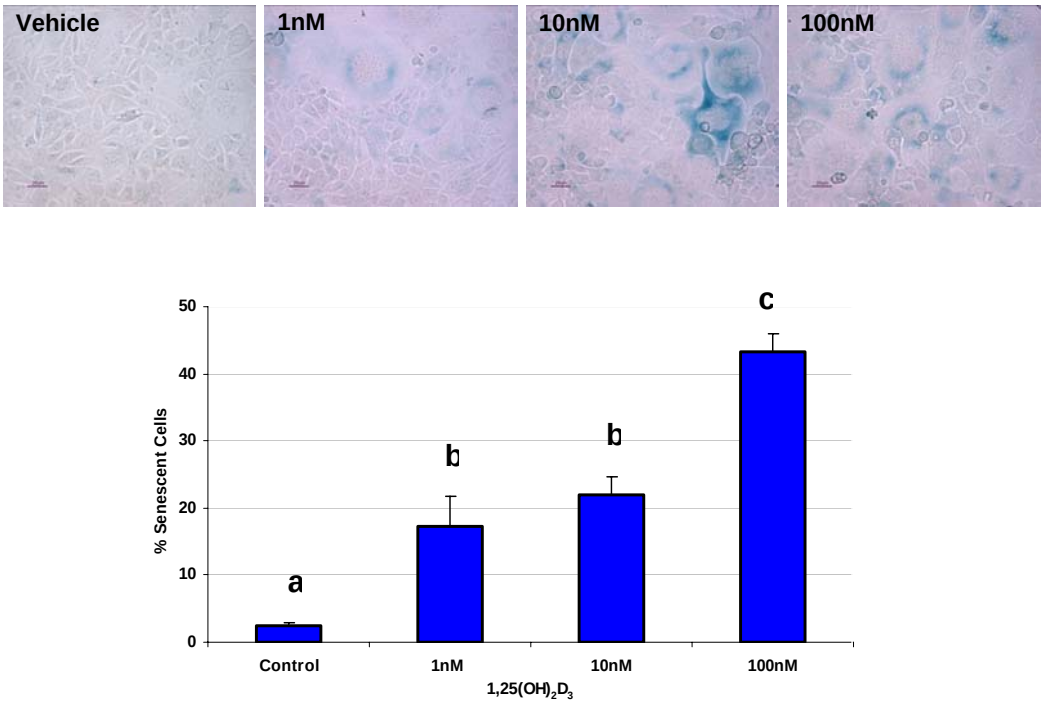

Means for n=10-20; ±SEM, $p<0.05$, Fisher's LSD Multiple Comparison

Figure P-3. Pten flox/flox MPEC and Pten-/- counterparts were treated with increasing concentrations of $1,25(OH)_2D_3$ and induction of senescence was determined by assessment of senescence-associated β-galactosidase activity. Cells treated with Doxorubicin were used as a positive control, while assessment of senescence at pH 7 in cells treated with Doxorubicin were used as a negative control.

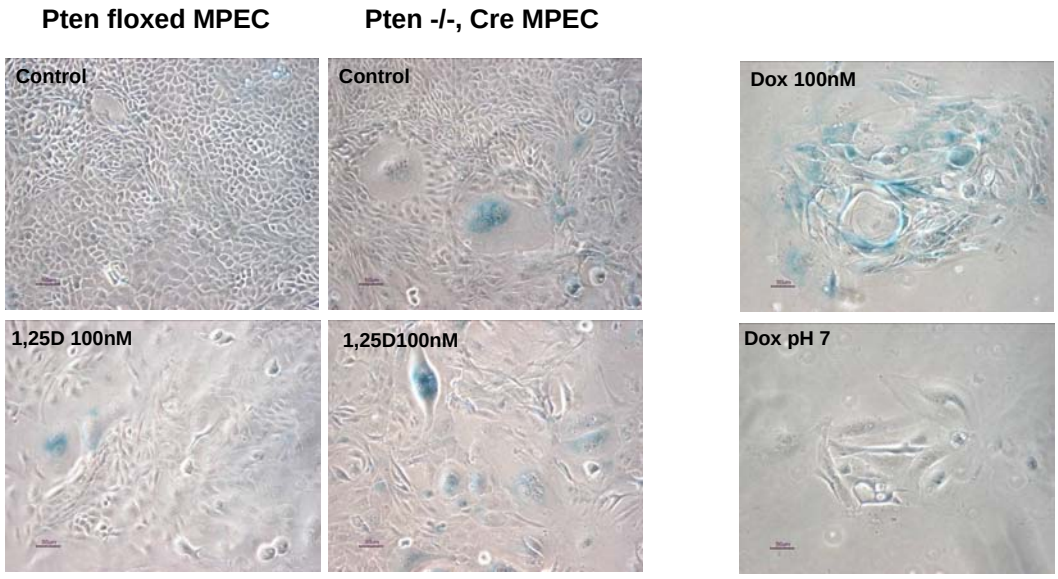

Figure P-4. MPEC WFU3 Control shRNA clone and respective WFU3 Pten shRNA clone were treated with increasing concentrations of $1,25(OH)_2D_3$ and induction of senescence was determined by assessment of senescence-associated β-galactosidase activity. Cells treated with Doxorubicin were used as a positive control, while assessment of senescence at pH 7 in cells treated with Doxorubicin were used as a negative control.

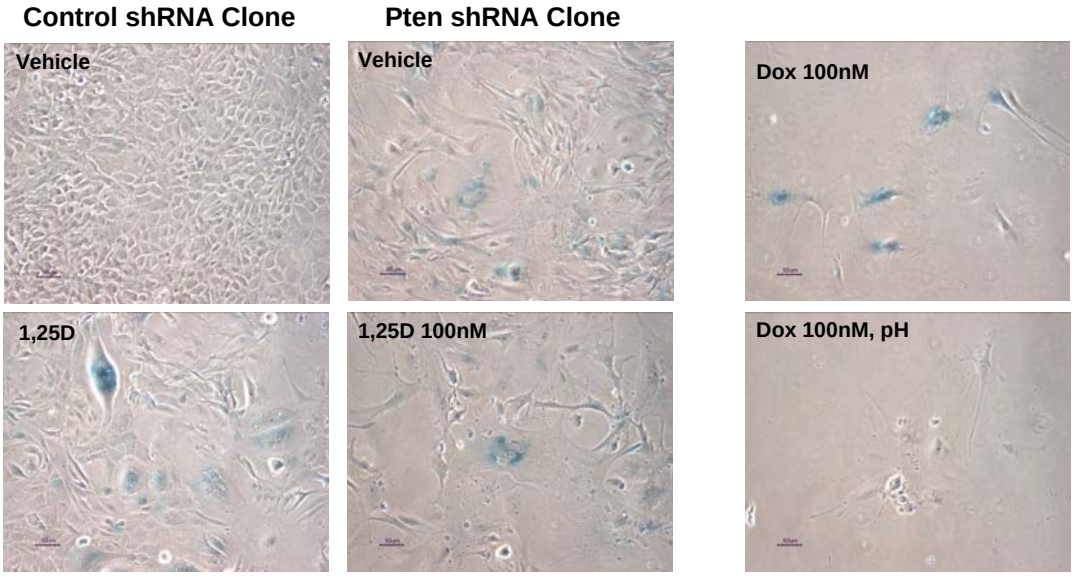

Key research accomplishments

- Manuscript is accepted for publication in Prostate journal (in press).
- Confirmed presence of synergism between AKT inhibitor API-2 and $1,25(OH)_2D_3$ in cells expressing Pten as well as cells that have lost Pten.
- Demonstrated cooperative induction of p21 by AKT inhibitor API-2 and $1,25(OH)_2D_3$ which might play role in cooperative induction of senescence by the two compounds.
- Have designed shRNA sequences targeting p21 and p27 in human cells and generated lentivirus that will allow knock down on the p21 and p27 protein in human cells.
- Preliminary data further confirms role of senescence in anti-proliferative qualities of $1,25(OH)_2D_3$.

Reportable outcomes

Altogether, we have demonstrated that pharmacological inhibitors of PI3K or Akt restored sensitivity to antiproliferative effects of $1,25(OH)_2D_3$ in $1,25(OH)_2D_3$-insensitive cells and synergized to inhibit the growth of Pten-/- mouse prostatic epithelial cells, DU145, LNCaP and primary human prostate cancer cell strains. The inhibitors used included API-2 (Triciribine) and GSK690693 which are currently in clinical trials for treatment of cancer. The combination of $1,25(OH)_2D_3$ and AKT inhibitor API-2 led to a cooperative increase in G_1 arrest and in the induction of senescence. AKT is commonly activated by PTEN loss, therefore we evaluated the role of Pten in responsiveness to $1,25(OH)_2D_3$ using shRNA knockdown and by *in vitro* knockout of Pten. We found that Pten status did not affect responsiveness to the antiproliferative action of $1,25(OH)_2D_3$.

In the past year we further developed the study and have demonstrated that in DU145 cells API-2 and $1,25(OH)_2D_3$ cooperated to induce p21 expression which may be associated with induction of senescence. In addition, we showed presence of this synergism in cells expressing Pten and in cells that have lost Pten. We found more pronounced synergism in cells with lower Pten expression (attached manuscript, Figure 6 and Table III).

Presently, we are working on confirmation of the ability of $1,25(OH)_2D_3$ (as well as $25(OH)D_3$ and cholecalciferol) to induce senescence in prostate cells and determination of the mechanism of this senescence. We are evaluating the role of Pten, p21, p27 for the induction of senescence by $1,25(OH)_2D_3$ (and potentially by $25(OH)D_3$ and cholecalciferol).

Conclusions

Altogether, we demonstrate that Pten status *per ce* did not affect responsiveness to the antiproliferative action of $1,25(OH)_2D_3$. We discovered that pharmacological inhibitors of PI3K or AKT are capable of restoring sensitivity to antiproliferative effects of $1,25(OH)_2D_3$ in $1,25(OH)_2D_3$-insensitive cells. In addition, the PI3K/AKT inhibitors tested synergized to inhibit the growth of Pten-/- mouse prostatic epithelial cells, DU145, LNCaP and primary human prostate cancer cell strains. Combination of $1,25(OH)_2D_3$ and AKT inhibitor cooperated to induce G_1 arrest, senescence, and p21 levels in prostate cancer cells.

As AKT is commonly activated by PTEN loss, we evaluated the role of Pten in responsiveness to $1,25(OH)_2D_3$ using shRNA knockdown and by *in vitro* knockout of Pten. MPEC that lost Pten expression remained sensitive to the antiproliferative action of $1,25(OH)_2D_3$, and showed higher degree of synergism between AKT inhibitor and $1,25(OH)_2D_3$ compared to Pten-expressing counterparts.

Inhibitors of the PI3K/AKT pathway included Triciribine and GSK690693 which are currently in clinical trials for treatment of cancer and the effect of the combination was 10 to 1000 times greater than the AKT inhibitor alone as was demonstrated by Dose Reduction Indexes. This synergistic effect has not been previously demonstrated and could significantly enhance the therapeutic efficacy of these clinically relevant drugs while reducing the potential side effects. Thus, these findings provide the rationale for the development of therapeutic interventions utilizing $1,25(OH)_2D_3$ or its analogs combined with inhibition of PI3K/AKT for the treatment of prostate cancer.

References:

1. Cancer Facts and Figures.: American Cancer Society, 2007.
2. Schwartz GG, Hulka BS. Is vitamin D deficiency a risk factor for prostate cancer? (Hypothesis). *Anticancer Res* 1990;10:1307-1311.
3. Ahonen MH, Tenkanen L, Teppo L, Hakama M, Tuohimaa P. Prostate cancer risk and prediagnostic serum 25-hydroxyvitamin D levels (Finland). *Cancer Causes Control* 2000;11:847-852.
4. Walters MR. Newly identified actions of the vitamin D endocrine system. *Endocr Rev* 1992;13:719-764.
5. Masumoto O, Ohyama Y, Okuda K. Purification and characterization of vitamin D 25-hydroxylase from rat liver mitochondria. *J Biol Chem* 1988;263:14256-14260.
6. Monkawa T, Yoshida T, Wakino S, Shinki T, Anazawa H, Deluca HF, Suda T, Hayashi M, Saruta T. Molecular cloning of cDNA and genomic DNA for human 25-hydroxyvitamin D3 1 alpha-hydroxylase. *Biochem Biophys Res Commun* 1997;239:527-533.
7. Hughes MR, Baylink DJ, Jones PG, Haussler MR. Radioligand receptor assay for 25-hydroxyvitamin D2/D3 and 1 alpha, 25-dihydroxyvitamin D2/D3. *J Clin Invest* 1976;58:61-70.
8. Clements MR, Davies M, Hayes ME, Hickey CD, Lumb GA, Mawer EB, Adams PH. The role of 1,25-dihydroxyvitamin D in the mechanism of acquired vitamin D deficiency. *Clin Endocrinol (Oxf)* 1992;37:17-27.
9. Banerjee P, Chatterjee M. Antiproliferative role of vitamin D and its analogs--a brief overview. *Mol Cell Biochem* 2003;253:247-254.
10. Rao A, Woodruff RD, Wade WN, Kute TE, Cramer SD. Genistein and vitamin D synergistically inhibit human prostatic epithelial cell growth. *J Nutr* 2002;132:3191-3194.
11. Peehl DM, Skowronski RJ, Leung GK, Wong ST, Stamey TA, Feldman D. Antiproliferative effects of 1,25-dihydroxyvitamin D3 on primary cultures of human prostatic cells. *Cancer Res* 1994;54:805-810.
12. Skowronski RJ, Peehl DM, Feldman D. Vitamin D and prostate cancer: 1,25 dihydroxyvitamin D3 receptors and actions in human prostate cancer cell lines. *Endocrinology* 1993;132:1952-1960.
13. Miller GJ, Stapleton GE, Hedlund TE, Moffat KA. Vitamin D receptor expression, 24-hydroxylase activity, and inhibition of growth by 1alpha,25-dihydroxyvitamin D3 in seven human prostatic carcinoma cell lines. *Clin Cancer Res* 1995;1:997-1003.
14. Zhao XY, Peehl DM, Navone NM, Feldman D. 1alpha,25-dihydroxyvitamin D3 inhibits prostate cancer cell growth by androgen-dependent and androgen-independent mechanisms. *Endocrinology* 2000;141:2548-2556.
15. Blutt SE, Weigel NL. Vitamin D and prostate cancer. *Proc Soc Exp Biol Med* 1999;221:89-98.
16. Ahmed S, Johnson CS, Rueger RM, Trump DL. Calcitriol (1,25-dihydroxycholecalciferol) potentiates activity of mitoxantrone/dexamethasone in an androgen independent prostate cancer model. *J Urol* 2002;168:756-761.
17. Getzenberg RH, Light BW, Lapco PE, Konety BR, Nangia AK, Acierno JS, Dhir R, Shurin Z, Day RS, Trump DL, Johnson CS. Vitamin D inhibition of prostate adenocarcinoma growth and metastasis in the Dunning rat prostate model system. *Urology* 1997;50:999-1006.
18. Krishnan AV, Peehl DM, Feldman D. Inhibition of prostate cancer growth by vitamin D: Regulation of target gene expression. *J Cell Biochem* 2003;88:363-371.
19. Cheng GZ, Park S, Shu S, He L, Kong W, Zhang W, Yuan Z, Wang LH, Cheng JQ. Advances of AKT pathway in human oncogenesis and as a target for anti-cancer drug discovery. *Curr Cancer Drug Targets* 2008;8:2-6.
20. Li DM, Sun H. PTEN/MMAC1/TEP1 suppresses the tumorigenicity and induces G1 cell cycle arrest in human glioblastoma cells. *Proc Natl Acad Sci U S A* 1998;95:15406-15411.
21. Li L, Ittmann MM, Ayala G, Tsai MJ, Amato RJ, Wheeler TM, Miles BJ, Kadmon D, Thompson TC. The emerging role of the PI3-K-Akt pathway in prostate cancer progression. *Prostate Cancer Prostatic Dis* 2005;8:108-118.
22. Rubin MA, Gerstein A, Reid K, Bostwick DG, Cheng L, Parsons R, Papadopoulos N. 10q23.3 loss of heterozygosity is higher in lymph node-positive (pT2-3,N+) versus lymph node-negative (pT2-3,N0) prostate cancer. *Hum Pathol* 2000;31:504-508.
23. Sansal I, Sellers WR. The biology and clinical relevance of the PTEN tumor suppressor pathway. *J Clin Oncol* 2004;22:2954-2963.
24. Sellers W, Sawyers CL. Somatic genetics of prostate cancer, oncogenes and tumor suppressors. In: Kantoff PW, Carroll PR, D'Amico AV, eds. Prostate Cancer: Principles and Practice. Philadelphia, PA: Lippencott, William & Wilkins, 2002.
25. Viglietto G, Motti ML, Bruni P, Melillo RM, D'Alessio A, Califano D, Vinci F, Chiappetta G, Tsichlis P, Bellacosa A, Fusco A, Santoro M. Cytoplasmic relocalization and inhibition of the cyclin-dependent kinase inhibitor p27(Kip1) by PKB/Akt-mediated phosphorylation in breast cancer. *Nat Med* 2002;8:1136-1144.
26. Kops GJ, de Ruiter ND, De Vries-Smits AM, Powell DR, Bos JL, Burgering BM. Direct control of the Forkhead transcription factor AFX by protein kinase B. *Nature* 1999;398:630-634.

27. Mamillapalli R, Gavrilova N, Mihaylova VT, Tsvetkov LM, Wu H, Zhang H, Sun H. PTEN regulates the ubiquitin-dependent degradation of the CDK inhibitor p27(KIP1) through the ubiquitin E3 ligase SCF(SKP2). *Curr Biol* 2001;11:263-267.
28. Andreu EJ, Lledo E, Poch E, Ivorra C, Albero MP, Martinez-Climent JA, Montiel-Duarte C, Rifon J, Perez-Calvo J, Arbona C, Prosper F, Perez-Roger I. BCR-ABL induces the expression of Skp2 through the PI3K pathway to promote p27Kip1 degradation and proliferation of chronic myelogenous leukemia cells. *Cancer Res* 2005;65:3264-3272.
29. Motti ML, Califano D, Troncone G, De Marco C, Migliaccio I, Palmieri E, Pezzullo L, Palombini L, Fusco A, Viglietto G. Complex regulation of the cyclin-dependent kinase inhibitor p27kip1 in thyroid cancer cells by the PI3K/AKT pathway: regulation of p27kip1 expression and localization. *Am J Pathol* 2005;166:737-749.
30. Zhou BP, Hung MC. Novel targets of Akt, p21(Cipl/WAF1), and MDM2. *Semin Oncol* 2002;29:62-70.
31. Campisi J, d'Adda di Fagagna F. Cellular senescence: when bad things happen to good cells. *Nat Rev Mol Cell Biol* 2007;8:729-740.
32. Michaloglou C, Vredeveld LC, Soengas MS, Denoyelle C, Kuilman T, van der Horst CM, Majoor DM, Shay JW, Mooi WJ, Peeper DS. BRAFE600-associated senescence-like cell cycle arrest of human naevi. *Nature* 2005;436:720-724.
33. Courtois-Cox S, Genther Williams SM, Reczek EE, Johnson BW, McGillicuddy LT, Johannessen CM, Hollstein PE, MacCollin M, Cichowski K. A negative feedback signaling network underlies oncogene-induced senescence. *Cancer Cell* 2006;10:459-472.
34. Schmitt CA, Fridman JS, Yang M, Lee S, Baranov E, Hoffman RM, Lowe SW. A senescence program controlled by p53 and p16INK4a contributes to the outcome of cancer therapy. *Cell* 2002;109:335-346.
35. Collado M, Gil J, Efeyan A, Guerra C, Schuhmacher AJ, Barradas M, Benguria A, Zaballos A, Flores JM, Barbacid M, Beach D, Serrano M. Tumour biology: senescence in premalignant tumours. *Nature* 2005;436:642.
36. Majumder PK, Grisanzio C, O'Connell F, Barry M, Brito JM, Xu Q, Guney I, Berger R, Herman P, Bikoff R, Fedele G, Baek WK, Wang S, Ellwood-Yen K, Wu H, Sawyers CL, Signoretti S, Hahn WC, Loda M, Sellers WR. A prostatic intraepithelial neoplasia-dependent p27 Kip1 checkpoint induces senescence and inhibits cell proliferation and cancer progression. *Cancer Cell* 2008;14:146-155.
37. Chen Z, Trotman LC, Shaffer D, Lin HK, Dotan ZA, Niki M, Koutcher JA, Scher HI, Ludwig T, Gerald W, Cordon-Cardo C, Pandolfi PP. Crucial role of p53-dependent cellular senescence in suppression of Pten-deficient tumorigenesis. *Nature* 2005;436:725-730.
38. Smith DC, Trump DL. A phase I trial of high-dose oral tamoxifen and CHOPE. *Cancer Chemother Pharmacol* 1995;36:65-68.
39. Gross C, Stamey T, Hancock S, Feldman D. Treatment of early recurrent prostate cancer with 1,25-dihydroxyvitamin D3 (calcitriol). *J Urol* 1998;159:2035-2039; discussion 2039-2040.
40. Schwartz GG, Whitlatch LW, Chen TC, Lokeshwar BL, Holick MF. Human prostate cells synthesize 1,25-dihydroxyvitamin D3 from 25-hydroxyvitamin D3. *Cancer Epidemiol Biomarkers Prev* 1998;7:391-395.
41. Flanagan JN, Young MV, Persons KS, Wang L, Mathieu JS, Whitlatch LW, Holick MF, Chen TC. Vitamin D metabolism in human prostate cells: implications for prostate cancer chemoprevention by vitamin D. *Anticancer Res* 2006;26:2567-2572.
42. Barclay WW, Woodruff RD, Hall MC, Cramer SD. A system for studying epithelial-stromal interactions reveals distinct inductive abilities of stromal cells from benign prostatic hyperplasia and prostate cancer. *Endocrinology* 2005;146:13-18.
43. Barclay WW, Axanova LS, Chen W, Romero L, Maund SL, Soker S, Lees CJ, Cramer SD. Characterization of adult prostatic progenitor/stem cells exhibiting self-renewal and multilineage differentiation. *Stem Cells* 2008;26:600-610.

ARTICLE PUBLISHED IN PROSTATE JOURNAL

1,25-dihydroxyvitamin D_3 and PI3K/AKT inhibitors synergistically inhibit growth and induce senescence in prostate cancer cells

Linara S. Axanova[1], Yong Q. Chen[1], Thomas McCoy[2], Guangchao Sui[1] and Scott D. Cramer[1, 2].

[1]*Cancer Biology and* [2]*Public Health Science Departments, Wake Forest University School of Medicine,* Medical Center Blvd.*, Winston Salem, NC 27157, U.S.A..*

Correspondence to: Scott D. Cramer, Department of Cancer Biology, Wake Forest University School of Medicine, Medical Center Blvd. Winston-Salem, NC 27157, U.S.A. scramer@wfubmc.edu

Key Words: Vitamin D_3, AKT, prostate, cancer, synergism

Running Title: Vitamin D_3 and AKT in prostate

Abstract: BACKGOUND: 1-alpha, 25-dihydroxy vitamin D_3 (1,25$(OH)_2D_3$) inhibits proliferation of multiple cancer cell types including prostate cells and upregulates p21 and/or p27, while loss of Pten and PI3K/AKT activation stimulates survival and downregulates p21 and p27. We hypothesized that inhibition of the PI3K/AKT pathway synergizes with the antiproliferative signaling of 1,25$(OH)_2D_3$. METHODS: Viability, cell cycle and senescence of cells were evaluated upon combinational treatment with 1,25$(OH)_2D_3$ and pharmacological PI3K/AKT inhibitors**.** RESULTS: Pharmacological inhibitors of PI3K or Akt and 1,25$(OH)_2D_3$ synergistically inhibited growth of DU145, LNCaP, primary human prostate cancer cell strains and Pten null mouse prostatic epithelial cells (MPEC). The inhibitors used included API-2 (Triciribine) and GSK690693 which are currently in clinical trials for treatment of cancer. A novel mechanism for antiproliferative effects of 1,25$(OH)_2D_3$ in prostate cells, induction of senescence, was discovered. Combination of 1,25$(OH)_2D_3$ and AKT inhibitor cooperated to induce G_1 arrest, senescence, and p21 levels in prostate cancer cells. As AKT is commonly activated by PTEN loss, we evaluated the role of Pten in responsiveness to 1,25$(OH)_2D_3$ using shRNA knockdown and by *in vitro* knockout of Pten. MPEC that lost Pten expression remained sensitive to the antiproliferative action of 1,25$(OH)_2D_3$, and showed higher degree of synergism between AKT inhibitor and 1,25$(OH)_2D_3$ compared to Pten-expressing counterparts. CONCLUSIONS: These findings provide the rationale for the development of therapies utilizing 1,25$(OH)_2D_3$ or its analogs combined with inhibition of PI3K/AKT for the treatment of prostate cancer.

Introduction

Prostate cancer is the most commonly diagnosed cancer and the second most common cause of cancer death in American men (1). Vitamin D deficiency has been associated with the development of clinical prostate cancer (2, 3).

Vitamin D is a hormone that can be obtained from the diet or produced endogenously by a series of reactions that culminate in the most active metabolite of vitamin D, 1α, 25$(OH)_2$-vitamin D_3 (1,25$(OH)_2D_3$). 1,25$(OH)_2D_3$ elicits antiproliferative effects in a variety of cancer cell types including cell lines derived from prostate (4, 5). The ability of 1,25$(OH)_2D_3$ to inhibit prostate growth was also demonstrated in primary prostatic cells from histologically normal, benign prostatic hyperplasia, and prostate cancer specimens6, in multiple prostate cancer cell lines (7-9), in xenograft models of prostate cancer (10, 11) as well as in Dunning rat prostate model (12). The anticancer mechanisms of 1,25$(OH)_2D_3$'s action include induction of cell cycle arrest, promotion of differentiation, inhibition of proliferation and angiogenesis, as well as inhibition of invasive and migratory potential of cancer cells (reviewed in 13).

Classical actions of 1,25$(OH)_2D_3$ are mediated through the vitamin D receptor (VDR) which is a member of a superfamily of nuclear steroid hormone receptors. Upon 1,25$(OH)_2D_3$ binding VDR translocates to the nucleus, dimerizes with retinoid X receptor (RXR) and modulates the expression of target genes. Although a number of 1,25$(OH)_2D_3$ responsive genes are known, the exact mechanism of growth regulation by 1,25$(OH)_2D_3$ is not completely defined; however, an increase in p21 and/or p27 is an almost universal feature (4).

One of the central contributing factors which facilitates the survival of prostate cancer cells is attributed to the phosphoinositol-3 kinase PI3K-AKT pathway. Activated AKT phosphorylates a host of proteins that affect cell growth, cell cycle entry, and cell survival. The AKT pathway presents an attractive target for anticancer therapies and several AKT inhibitors have been developed that demonstrate anticancer activity in preclinical and clinical studies (14). In prostate cancer, activation of AKT occurs most frequently due to the loss of tumor suppressor phosphatase and a tensin homologue deleted in chromosome ten (PTEN) (15-17). Loss of PTEN protein occurs in 20% of primary prostate tumors and this loss is highly correlated with advanced tumor grade and stage with 50% of metastatic tumors exhibiting a loss of PTEN protein (18). Moreover, loss of heterozygosity (LOH) is found in 20%

to 60% of metastatic tumors (19)**.** Data suggests that advancing disease is associated with a progressive loss of PTEN or an accumulation of mutations in the PTEN gene. Loss of PTEN and activation of AKT has been shown to downregulate the expression of p21 and p27 by a number of mechanisms (20-24). Since the antiproliferative effects of 1,25$(OH)_2D_3$ involve upregulation of p21 and/or p27 4 while activation of PI3K/AKT downregulates their expression (24), we hypothesized that pharmacological inhibitors of AKT will cooperate with the antiproliferative actions of 1,25$(OH)_2D_3$ in prostate cancer cells.

Our results demonstrate that inhibition of PI3K or AKT synergized with 1,25$(OH)_2D_3$ to inhibit the growth of human prostate cancer cell lines and primary human prostate cancer strains, and led to the cooperative induction of G_1 arrest and senescence. Responsiveness to the antiproliferative effects of 1,25$(OH)_2D_3$ was not lost upon reduction of Pten expression or its deletion. We observed a higher susceptibility to synergism between 1,25$(OH)_2D_3$ and AKT inhibitor in MPECs with lost Pten expression compared to the cells expressing Pten. These findings provide the rationale for prostate cancer therapies involving use of AKT inhibitors and 1,25$(OH)_2D_3$ in adjunctive therapy.

Materials and Methods

Materials. 1,25$(OH)_2D_3$ (Biomol, Plymouth Meeting, PA) was reconstituted in 100% ethanol and stored at -80ºC. LY294002 (Sigma-Aldrich Co., St Louis, MO), GSK690693 (26) (a generous gift from GlaxoSmithKline, Collegeville, PA) and API-2 (27) (Calbiochem, La Jolla, CA) were reconstituted in DMSO and stored at -20ºC.

shRNA Infection. WFU3 MPEC (25) were infected with lentivirus expressing shRNA targeting Pten (gaa cct gat cat tat aga tat t) or control shRNA (gggc cat ggc acg tac ggc aag). Lentivirus production and infection procedure were previously described (26). MPEC were clonally selected using serial dilution as described (27) and Pten status was confirmed by Immunoblot.

MPECs with acute deletion of Pten: Prostate-specific Pten-knockout mice were generated by crossing $Pten^{loxP/loxP}$ mice (28) with mice of the ARR2Probasin-cre transgenic line PB-cre4, wherein the Cre recombinase is under the control of a modified rat prostate-specific probasin promoter (22), as previously reported (29). $Pten^{lox/lox}$ anterior mouse prostatic epithelial cells (MPECs) were isolated from 8 week old $Pten^{lox/lox;\ pbCre-}$ animals as described (25) and infected with self-deleting Cre-recombinase lentivirus ($Pten^{-/-}$) (30). Deletion was validated by PCR and Immunoblot.

Tissue culture. LNCaP and DU145 cells (both from American Type Culture Collection, Manassas, VA) were grown in RPMI-1640 supplemented with 10% FBS and 1% Penicillin-Streptomycin. MPEC were grown as described previously (25). Human prostate epithelial cancer cell strain WFU273Ca was isolated from fresh human prostate (prostate cancer, Gleason grade 6) validated for histological origin and maintained as previously described (31). Acquisition of the human specimen from radical prostatectomies was performed at Wake Forest University School of Medicine in compliance with Institutional Research Board approval. Briefly, a small piece of tissue was removed and minced. The tissue was digested with collagenase overnight. To remove the collagenase and the majority of the stromal cells, the tissue was rinsed and centrifuged. The tissue was inoculated into a tissue culture dish coated with collagen type I (Collagen Corporation, Palo Alto, CA) and grown in medium PFMR-4A (32) supplemented with growth factors and hormones as described (31). The histology of each specimen was verified by inking and fixing the prostate after dissection and serially sectioning the marked area as well as the sections immediately adjacent to the area of the dissection. The cells that grew out from the

tissue were aliquoted and stored in liquid nitrogen. The frozen aliquots were thawed to produce secondary cultures, which were grown in medium MCDB 105 (Sigma, St. Louis, MO) supplemented with growth factors and hormones as described (31).

Growth assays for synergism determination. Cells were plated at 10^4 cells per 35 mm dish in triplicate. To determine synergism cells were treated with increasing doses of AKT inhibitor, increasing doses of $1,25(OH)_2D_3$ or multiple combinations of AKT inhibitor and $1,25(OH)_2D_3$. Briefly, 48 hr after plating the cell growth medium was replaced with 1 ml of experimental medium containing twice (2x) the indicated concentration of a PI3K/AKT inhibitor or vehicle (DMSO, 1x = 0.1% V/V). One hour later 1 ml of medium containing twice the final concentration of $1,25(OH)_2D_3$ or vehicle (ethanol, 1x = 0.1% V/V) was added to each dish. An AKT inhibitor was applied 1 hour prior to the $1,25(OH)_2D_3$ treatment as API-2 was shown to reduce phosphorylation of AKT and phosphorylation of AKT's downstream targets (Bad, AFX, and GSK-3ß) as early as at 1 hour post treatment (33). In addition, our preliminary tests demonstrated that application of AKT inhibitor 1 hr prior to $1,25(OH)_2D_3$ treatment demonstrated moderately stronger synergism of growth inhibition compared to 0 hr, 4 hr, 8 hr and 24 hr between the treatments (data not shown).

DU145, LNCaP cells and MPEC remained in the experimental medium until the vehicle control cells reached 80-90% confluence, typically 5-7 days. For WFU273Ca and for all experiments using GSK690693 the experimental medium was replaced every 48hr. Viable cells were counted with a hemacytometer after trypan blue exclusion. Results of representative experiments are shown.

Flow cytometry: Flow cytometry was performed as described (5) using Becton Dickinson FACSCaliber and analyzed by the Cell Quest Pro v.6.0 program (Becton Dickinson, Mansfiled, MA). Data were processed with ModFit LT v.2.0 software (Verity Software House, Topsham, MN). Each treatment was performed in triplicate and the experiment was conducted three times.

Senescence-associated (SA)-β-galactosidase (gal) activity: Cells were cultured and treated as described above. After 5-7 days of treatment (SA)-β-galactosidase activity was evaluated by the method of Dimri et al. (34). For positive control SA-β-gal activity was evaluated in cells treated with 100

nM Doxorubicin; for negative control SA-β-gal activity was evaluated in cells treated with 100 nM Doxorubicin at pH 7 which inhibits SA-β-gal activity. Digital images were taken from 10 random areas at 20X magnification. Digital images were evaluated in Photoshop CS2 9.0.2 (Adobe Systems, San Jose, CA). The number of SA-β-gal positive cells was counted in each image and presented as percent of total cell number ± SE.

Immunoblot: Cells were collected from monolayer by light trypsinization and cell pellets were resuspended in lysis buffer (20 mM HEPES, 10 mM NaCl, 3 mM $MgCl_2$, 0.1% NP40, 10% glycerol, 0.2 mM EDTA) containing freshly added 1 mM DTT and 0.4 mM PMSF. Tubes with cells were left on ice for 15min. 50µg of protein were subjected to electrophoresis on SDS-PAGE gels. Proteins were transferred onto prewetted Hybond-P PVDF (polyvinylidene diflouride) membrane according to manufactures' protocol (Amersham Pharmacia Biotech, Buckinghamshire, UK). Membranes were incubated with appropriate dilutions of Pten (sc-7974) (Santa Cruz Biotechnology, Santa Cruz, CA), p21 (556430) and p27 (610241) antibodies (BD Pharmigen**,** San Diego, CA). Secondary antibodies conjugated to horse radish peroxidase (Santa Cruz Biotechnology) were used. ECL Plus Western Blotting Detection System kit (Amersham-Pharmacia) was used for detection of proteins. Images were analyzed by ImageQuant TL v. 7.0 (GE Healthcare, Piscataway, NJ).

Detection of phosphorylated proteins: Cells were grown to approximately 80% confluency, medium was replaced with fresh medium, and in 24hr protein lysates were prepared. Cells were washed with cold PBS and lysis buffer (1%NP-40, 50mM Tris-Hcl, 150mM NaCl, 5mM EDTA with freshly added protease inhibitor cocktail, 100mM DTT, 100mM Na_3VO_4 and 500mM NaF) was applied. Cells were left on ice for 20min, collected, and centrifuged. Supernatants were stored at -80°C. 30-50µg of protein were subjected to electrophoresis on SDS-PAGE gels. Proteins were transferred onto Nitrocellulose membrane (Bio-Rad Laboratories, Hercules, CA) according to the manufacturer's protocols. Membranes were incubated with appropriate dilutions of pSer473 AKT (#4051), pThr308 AKT (#2965), AKT (#9272) antibodies (Cell Signaling Inc., Beverly, MA). Secondary antibodies conjugated to horse radish peroxidase (Santa Cruz Biotechnology) were used. Protein expression

levels were detected using ECL Plus Western Blotting Detection System kit (Amersham-Pharmacia). Images were analyzed by ImageQuant TL v. 7.0 (GE Healthcare, Piscataway, NJ).

Statistical Analyses: Synergism was assessed with CalcuSyn software (Biosoft, Ferguson, MO) as previously described (5). Briefly, the dose effect for each drug alone was determined based on the experimental observations using the median effect principle: the combination index (CI) for each combination was calculated according to the following equation: $CI = [(D)_1/(D_x)_1] + [(D)_2/(D_x)_2] + [(D)_1(D)_2/(D_x)_1(D_x)_2]$, where $(D)_1$ and $(D)_2$ are the doses of drug that have *x* effect when used in combination and $(D_x)_1$ and $(D_x)_2$ are the doses of drug 1 and drug 2 that have the same *x* effect when used alone. CI = 1 represents the conservation isobologram and indicates additive effects. CI values < 1 indicate a more than expected additive effect (synergism). Dose Reduction Index (DRI) for each drug and dose was calculated using the equation: $(DRI)_1=(D_x)_1/D_1$ and $(DRI)_2=(D_x)_2/D_2$.

Statistical analyses for synergism experiments were performed using the statistical software package NCSS 2002 (Number Cruncher Statistical Systems, Kaysville, UT). Differences in growth data were determined by two-way ANOVA controlling for $1,25(OH)_2D_3$ or PI3K/AKT inhibitor dose with post hoc analysis by Fisher's test. Cell cycle distribution and senescence analyses were performed using two-way ANOVA with post hoc analysis by Fisher's LSD test. In all cases, $P \leq 0.05$ was considered significant. The effect of $1,25(OH)_2D_3$-mediated growth inhibition in MPECs with Pten shRNA and scrambled control or $Pten^{-/-}$ and $Pten^{lox/lox}$ was evaluated using two-way ANOVA while adjusting for the within-clone correlation using a random effect in a corresponding mixed-effects model. Data were analyzed in PROC MIXED in SAS v9.2.

Results

$1,25(OH)_2D_3$ and PI3K/Akt inhibitors synergistically inhibit prostate cancer cell growth.

To test whether inhibition of the PI3K/Akt pathway synergizes with $1,25(OH)_2D_3$ treatment to inhibit the growth of prostatic cells we first utilized a pharmacological inhibitor of PI3K/AKT, LY294002 (35). Cells were treated with increasing doses of $1,25(OH)_2D_3$ or LY294002 or with multiple combinations of the two compounds and the number of viable cells was assessed. This was followed by assessment of synergism using the Chou-Talalay method (36) in which the combination index (CI) values < 1 indicates presence of synergism.

We found that LNCaP cells, which lack functional PTEN and are moderately sensitive to growth inhibition by $1,25(OH)_2D_3$, demonstrated statistically significant synergism between $1,25(OH)_2D_3$ and LY294002 at lower doses of $1,25(OH)_2D_3$ (Fig. 1A, Table I). The combination of 1 nM $1,25(OH)_2D_3$ - treatment with 0.2 μM, 1 μM or 5 μM LY294002 demonstrated statistically significant synergism as determined by CI values from isobologram analysis (Table I). The dose-reduction index (DRI) for each of the drugs is also depicted in Table I and presents a predictive measure of how much the dose of each drug in a synergistic combination may be reduced at a given effect level compared with the doses of each drug alone (36).

DU145 cells (wild-type PTEN) are known to be resistant to the antiproliferative effects of $1,25(OH)_2D_3$ (37). Consistent with this, we found that $1,25(OH)_2D_3$ did not significantly affect growth of DU145 cells (Fig. 1B). While 100 nM $1,25(OH)_2D_3$ did not inhibit growth of DU145 cells, pretreatment of DU145 cells with 5 μM LY294002 sensitized the cells to $1,25(OH)_2D_3$ treatment leading to a reduction in the number of viable cells to 40% compared to treatment with LY294002 alone (Fig.1B). Significant synergism was observed across multiple doses of both compounds (Table I).

As LY294002 has recently been reported to have many other off-target effects (38), we sought to validate synergism with AKT-inhibition specifically. To do so we used two different AKT inhibitors which currently are in clinical trials for cancer treatment: API-2 (Triciribine), which selectively inhibits Akt1/2/3 without inhibiting PI3K or PDK (33) and GSK690693, an ATP competitive AKT inhibitor (39).

The combination of 1,25$(OH)_2D_3$ with API-2 elicited synergistic growth inhibition of DU145 cells (Fig. 2A, Table II). DU145 cells treated with the combination of API-2 and 1,25$(OH)_2D_3$ demonstrated strong synergism at all doses tested as determined by CI values from isolobolgrams (Table II). Noteworthy, the treatment with API-2 and 1,25$(OH)_2D_3$ was applied only once after which the cells were allowed to grow until the cells in either of the treatment groups were 80-90% confluent.

Next we tested for the presence of synergism in primary human prostate cancer epithelial cells. WFU273Ca human primary epithelial cell strain was isolated from fresh human prostate with histologically confirmed prostate cancer of Gleason grade 6. The strain was shown to be PTEN-positive by Immunoblot, while still demonstrating high levels of activated phosphorylated AKT (Fig. 2B, insert). The combination of API-2 and 1,25$(OH)_2D_3$ applied to WFU273Ca strain also demonstrated statistically significant synergism (Fig. 2B, Table II), with DRI values as high as 15.3 for 1,25$(OH)_2D_3$ and 14.6 for API-2.

Even though both cell types, the WFU273Ca cell strain and DU145 cell line, are PTEN-positive, WFU273Ca shows activation of AKT pathway as demonstrated by phospho-AKT levels (Fig.2B, insert) while DU145 consistently demonstrated undetectable levels of pAKT (data not show). The mechanistic basis for activated AKT in WFU273Ca is not known. The higher sensitivity of the WFU273Ca cell line to growth inhibition by AKT inhibitor API-2 might be explained by possible dependency of WFU273Ca on AKT activation for proliferation of the cells.

The combination of GSK690693 with 1,25$(OH)_2D_3$ also elicited strong to very strong synergistic growth inhibition in DU145 cells (Fig. 2C, Table II), as well as moderate to very strong synergism in human primary prostatic epithelial cells (Fig. 2D, Table II).

1,25$(OH)_2D_3$ and PI3K/Akt inhibitors cooperate to inhibit cell cycle progression and induce senescence

Having demonstrated synergism between 1,25$(OH)_2D_3$ and AKT inhibitors we sought to explore the mechanism. First, we performed video time-lapse microscopy analysis of DU145 cells treated with API-

2 (0.25 μM) or 1,25$(OH)_2D_3$ (100 nM) alone as well as in combination of the two. We did not observe any considerable apoptosis in either of the treatments (data not shown). Next we evaluated cell cycle distribution of DU145 cells treated with API-2 or 1,25$(OH)_2D_3$. Cell cycle analysis demonstrated a small but statistically significant increase in G_1-arrested cells treated with the combination of API-2 at 0.25 μM with 1,25$(OH)_2D_3$ at 10 nM compared to either agent alone (Fig. 3).

When we assessed the effects of drug combination on senescence in the human primary prostate cancer cell strain WFU273Ca, we found that 1,25$(OH)_2D_3$ was able to induce SA-β-Gal activity which was associated with morphological features consistent with senescence (Fig. 4A, B). Interestingly, inhibition of the AKT pathway with API-2 alone induced senescence in WFU273Ca cells with 0.5μM API-2 causing 30% of the cells to undergo senescence, suggesting a role for activated AKT in the prevention of senescence in these cells (Fig. 3C). The combination of API-2 and 1,25$(OH)_2D_3$ cooperated to induce greater SA-β-Gal activity which was statistically significant by ANOVA (Fig. 3D). Treatment with 0.1 μM API-2 induced senescence in 6.5% of WFU273Ca cells and 10 nM 1,25$(OH)_2D_3$ induced senescence in 7.3% of the cells; while the combination of the two led to 24.0% of the cells to undergo senescence (Fig. 3D). DU145 cells also showed cooperativity for induction of SA-β-gal (Fig. 3E).

As the antiproliferative effects of 1,25$(OH)_2D_3$ commonly involve upregulation of $p21^{Cip1}$ and/or $p27^{Kip1}$ (4) we sought to test the effect of AKT inhibition and 1,25$(OH)_2D_3$ treatment on protein levels of $p21^{Cip1}$ and $p27^{Kip1}$ in DU145. The result demonstrated that 24hr of treatment with API-2 and 1,25$(OH)_2D_3$ cooperated to increase $p21^{Cip1}$ protein (Fig. 3F). While 0.25μM API-2 treatment increased p21 by 3.7 fold and 100nM 1,25$(OH)_2D_3$ did not have a significant effect, the combination of the two led to an 8.3 fold increase in the $p21^{Cip1}$ protein level compared to the base level. Although API-2 treatment modestly increased p27 levels, 1,25$(OH)_2D_3$, alone or in combination with API-2 did not demonstrate a significant effect on p27 protein levels.

Together these data suggest that synergism between API-2 and 1,25$(OH)_2D_3$ in prostate cancer cells might be a result of cooperative induction of cell cycle arrest and senescence possibly through induction of $p21^{Cip1}$ levels.

The role of Pten status in sensitivity to antiproliferative action of $1,25(OH)_2D_3$.

Activation of AKT in prostate cancer occurs most frequently due to the loss of the tumor suppressor phosphatase and a tensin homologue deleted in chromosome ten (PTEN), which is found in 20% of primary tumors and more than 50% of metastatic tumors (18). Thus, we wanted to evaluate the role of Pten in the antiproliferative signaling of $1,25(OH)_2D_3$. To test this we generated MPEC in which Pten expression was suppressed using an shRNA approach. MPEC WFU3 (25) were infected with either lentivirus expressing scrambled shRNA or with lentivirus expressing shRNA targeting Pten. Single cell clones of each of the cell types were established and Pten status was verified by Immunoblot (Fig.5B). All clones with Pten expression knocked down to undetectable levels were selected and activation of Akt pathway was confirmed by assessment of Akt phosphorylation. Clones infected with Pten shRNA activated Akt pathways as phospho-Ser473 and phospho-Thr308 Akt levels were increased compared to the Control clones (Fig.5B).

WFU3 control MPEC clones and WFU3 MPEC clones with Pten knocked down were treated with increasing doses of $1,25(OH)_2D_3$ (Fig.5A). Both cell types exhibited robust growth suppression by $1,25(OH)_2D_3$ in a dose-dependant manner. There was a trend towards increased sensitivity of Pten shRNA clones to $1,25(OH)_2D_3$-mediated growth inhibition at 10nM dose ($p=0.041$) but not at 100nM ($p=0.655$) as shown by two-way ANOVA. The overall test for any differences (across Ethanol, 10nM, 100nM) in Control and Pten shRNA clones was not significant ($p=0.089$). These findings demonstrate that loss of Pten expression and activation of Akt pathway doesn't reduce responsiveness of the cells to the antiproliferative effects of $1,25(OH)_2D_3$ and suggests a possible increase in the sensitivity of the cells with lost Pten to the antiproliferative actions of $1,25(OH)_2D_3$.

Since gene suppression using an shRNA approach has the potential disadvantages of incomplete suppression of target gene expression and also possible off-target effects, we sought to establish a cell line with acute *in vitro* deletion of Pten. Thus, we isolated $Pten^{lox/lox}$ MPEC from prostates of $Pten^{lox/lox}$ Cre-recombinase negative animals and infected them with lentivirus expressing self-deleting Cre-recombinase (30). PCR analysis (data not shown) and Immunoblot analysis (Fig. 5D) demonstrated the absence of Pten expression in the cells infected with Cre-recombinase. Deletion of Pten led to 5.6 fold increase in phosphor-Ser473 Akt level confirming activation of the Akt pathway (Fig. 5D). The control

Pten$^{lox/lox}$ MPEC and Pten$^{-/-}$ (Pten$^{lox/lox}$ infected with Cre-recombinase lentivirus) cells were treated with increasing concentrations of 1,25$(OH)_2D_3$. We observed that *in vitro* loss of Pten did not significantly affect the ability of 1,25$(OH)_2D_3$ to inhibit the growth of the cells (Fig. 5B).

Pten$^{lox/lox}$ MPEC demonstrated higher sensitivity to 1,25$(OH)_2D_3$ compared to WFU3 MPEC used for the shRNA knock down of Pten. This could be attributed to the difference in the genetic background of the mouse strains from which the cell lines were established. The WFU3 MPECs used for the infection with shRNA-expressing virus were isolated from prostates of B1/6; 129/SVEV mice (25), while Pten$^{lox/lox}$ MPEC were isolated from mice of mixed C57BL/6 and BALB/c background (40, 29).

We also evaluated the effect of Pten status on the presence of synergism between 1,25$(OH)_2D_3$ and AKT inhibitor API-2. WFU3 Control clone 3 MPEC (the clone with the lowest levels of phosphor-Ser473 Akt) and WFU3 Pten shRNA clone 4 MPEC (the clone with the highest levels of phospho-Ser473 Akt and phosphor-Thr308 Akt) were treated with 1,25$(OH)_2D_3$ (0.1nM, 1nM, 10nM, and 100nM) or API-2 (10nM, 50nM, 100nM, and 500n) or with multiple combinations of the two compounds. Out of all dose combinations tested the control clone MPEC showed “intermediate” synergism at 10nM 1,25$(OH)_2D_3$ combined with 50nM or 100nM API-2 (Fig.5A, Table III). On the other hand, MPEC with Pten knock down showed “*very strong”* to *“strong”* synergism throughout all tested dose combinations of 1,25$(OH)_2D_3$ and API-2 as determined by the CI values (Fig. 5B, Table III). A similar trend was observed in the MPEC with Pten deleted using Cre-recombinase. Briefly, Pten$^{lox/lox}$ MPEC demonstrated only “intermediate” synergism between 1,25$(OH)_2D_3$ and API-2 at 10nM 1,25$(OH)_2D_3$ combined with 5nM and 50nM API-2, while the Pten$^{-/-}$ MPEC demonstrated “strong” to “very strong” synergism at the highest dose of API-2 tested (500nM) combined with any dose of 1,25$(OH)_2D_3$ (data not shown).

Together, these data demonstrate that suppression or loss of Pten in MPECs was not associated with increased resistance to growth-inhibitory qualities of 1,25$(OH)_2D_3$ in MPEC. In addition, our data suggests that loss of Pten might strengthen the synergistic effect between 1,25$(OH)_2D_3$ and AKT inhibition on cellular growth inhibition.

Discussion

In this study we showed that AKT inhibitors in combination with $1,25(OH)_2D_3$ synergistically inhibit the growth of prostate cancer cells. The effect was observed with multiple inhibitors of PI3K and/or AKT in MPEC with Pten knock down, prostate cancer cell lines, as well as primary human prostate cancer sample.

These findings might be important as AKT inhibitors (including the ones tested in this study) are in clinical trials for various cancers (14,26,50), and therefore the results could have fast clinical translation. However, a factor complicating the use of AKT inhibitors is that the AKT pathway presents one of the most important pathways for normal cell survival. It is not clear yet whether treatment with AKT inhibitors will demonstrate acceptable levels of toxicity at doses that are therapeutically effective.

$1,25(OH)_2D_3$ used as a single agent has been shown to possess anticancer qualities in a number of cancer models but has toxicities associated with calcium mobilization at doses that are therapeutically effective (4). One strategy to overcome this problem is the creation of less calcemic $1,25(OH)_2D_3$ analogs or organization of the treatment regimen in a way that allows reduction of side-effects. Another strategy is to combine $1,25(OH)_2D_3$ with other agents to develop therapeutic interventions that allow dose reduction, and thus alleviation of toxicities, while maintaining the growth inhibitory potential. Clinical trials utilizing $1,25(OH)_2D_3$ or its analogs in combination with chemotherapy in advanced prostate cancer have demonstrated the feasibility of the use of $1,25(OH)_2D_3$ for treatment of advanced prostate cancer (51-53). For instance, Beer et al. reported an 81% response rate for the combination of $1,25(OH)_2D_3$ and docetaxel in metastatic prostate cancer versus an expected response of 40% to 50% for docetaxel alone (41).

In this light, synergism between $1,25(OH)_2D_3$ with AKT inhibitors and DRI values demonstrated in this study suggests that more therapeutic efficacy can be achieved by combining AKT inhibitors and $1,25(OH)_2D_3$ (or its analogs) potentially reducing systemic toxicities.

Mechanistically, combinational treatment with AKT inhibitor and $1,25(OH)_2D_3$ showed no evidence of apoptosis, but moderate effect on cell cycle progression and larger effect on the induction of senescence was observed.

Treatment with 1,25$(OH)_2D_3$ alone did not have an effect on senescence in DU145 cells which is in agreement with the observation that these cells are not growth-inhibited by 1,25$(OH)_2D_3$. However, combined with AKT inhibitor API-2, 1,25$(OH)_2D_3$, increased the percentage of cells undergoing senescence.

In human primary prostate cancer cell strain treatment with 1,25$(OH)_2D_3$ alone was able to inhibit proliferation of the cells as well as to induce senescence as demonstrated by induction of β-galactosidase straining and senescence-associated cell morphology alterations. The ability of 1,25$(OH)_2D_3$ to induce senescence in prostate cells has *not* been demonstrated before and contributes to the understanding of the antiproliferative effects of 1,25$(OH)_2D_3$ in prostate cells which have not been clearly defined.

Senescent cells are described as a cell permanently arrested in the cell cycle. These cells are refractory to proliferation stimuli, exhibit altered cell morphology and gene expression while remaining viable and preserving metabolic activity (reviewed in ((42). There are multiple data demonstrating that senescence is a mechanism that limits cellular lifespan and presents a barrier for cellular immortalization and progression of tumorigenesis (43, 44). DNA damage or oncogene expression can induce cellular senescence and in order to become immortal cells have to overcome senescence by acquiring additional genetic alterations.

A process of senescence was demonstrated to have a significant role in human cancers as well. It was shown that human benign tumors contain senescent cells and that these cells disappear in their malignant counterparts (45, 46). In human prostate cancer Majumder et al. (47) demonstrated that markers of cellular senescence are elevated in PIN when compared to nondysplastic elithelial cells in the same tissue section. Chen et al. (48) showed that in specimens from early-stage human prostate cancer markers of senescence were present in areas of prostate hyperplasia/PIN and rarely in areas of carcinoma. These findings suggest a role for senescence as a barrier for progression of tumorigenesis in prostatic cells. The ability of 1,25$(OH)_2D_3$ to induce senescence in human primary prostate cancer cell strain demonstrated in the study supports utilization of 1,25$(OH)_2D_3$ for the treatment of earlier stages of human prostate cancer with the goal of prevention of disease progression. Ultimately, combination of 1,25$(OH)_2D_3$ with pharmacological AKT inhibitors might provide further benefits by stimulation of senescence, reduction of growth of cancer cell and blocking or slowing tumorigenesis.

It was previously demonstrated that p21or p27 expression plays a critical role in the induction of senescence in a number of cell types (49-51) including prostate cells (47). In addition, 1,25$(OH)_2D_3$ has been shown to increase the steady-state levels of p27 protein in prostate cancer cells (52). Thus, we sought to explore the effect of AKT inhibition and 1,25$(OH)_2D_3$ treatment on the p21 and p27 levels. In agreement with the lack of response to antiproliferative action of 1,25$(OH)_2D_3$ DU145 that did not induce p21, p27 levels upon 1,25$(OH)_2D_3$ treatment. However, when AKT inhibitor API-2 induced p21 protein levels, the cooperative induction of p21 by the combinational treatment with API-2 and 1,25$(OH)_2D_3$ was observed, which correlated with sensitization of the cells to the antiproliferative effects of 1,25$(OH)_2D_3$ and induction of senescence. Thus, while 1,25$(OH)_2D_3$-*sensitive* cell strains undergo senescence upon 1,25$(OH)_2D_3$ treatment, the 1,25$(OH)_2D_3$-*insensitive* DU145 cell line required an AKT inhibitor treatment in order for 1,25$(OH)_2D_3$ to inhibit proliferation and induce senescence.

As activation of AKT in prostate cancer commonly occurs due to the loss of expression of functional PTEN (18), we evaluated the role of Pten in responsiveness to 1,25$(OH)_2D_3$, as well as the role of Pten in synergistic cell growth inhibition upon treatment with 1,25$(OH)_2D_3$ in combination with AKT inhibitors.

We demonstrated that loss of Pten in MPEC was not associated with decreased responsiveness of the cells to antiproliferative effects of 1,25$(OH)_2D_3$. There was a suggestion for increased sensitivity of cells with deleted Pten to lower dose of 1,25$(OH)_2D_3$ tested (10nM) as shown by slightly higher growth inhibition of MPEC clones with Pten knocked down using shRNA compared to the Control MPEC clones at that dose ($p=0.041$).

More profound synergism between 1,25$(OH)_2D_3$ and AKT inhibitor API-2 was observed in MPEC that lost Pten expression as compared to the Pten-expressing counterparts. This finding, if confirmed by further studies, could be relevant to clinical application as cancer cells with lost Pten would be more sensitive to the growth-inhibitory effects of the combinational treatment leading to more selective growth inhibition of prostate cancer cells. However, in human prostate cancer cell lines synergism was observed in cells with functional Pten (DU145), as well as in cells lacking Pten activity (LNCaP). Thus, role of Pten status for the induction of synergism might be cell-type specific.

Conclusions

In summary, our results show that $1,25(OH)_2D_3$ and AKT inhibitors synergistically inhibit prostate cancer growth through induction of cell cycle and senescence. We also have demonstrated that reduced Pten expression was *not* associated with decreased response to antiproliferative actions of $1,25(OH)_2D_3$ suggesting that $1,25(OH)_2D_3$ can be used for treatment independent of PTEN status of the tumor. These data may have implications for the clinical use of these agents in prostate cancer patients especially in patient with high risk for progression.

Acknowledgement

We are grateful to GlaxoSmithKline (Collegeville, PA) which generously provided GSK690693 used in the study. We thank Dr.George Kulik (Department of Cancer Biology, Wake Forest University School of Medicine) for providing us with API-2. Authors declare to have no financial or personal relationship which may inappropriately influence the presentation of this work.

Figure Legends

Figure 1. LY294002 and 1,25(OH)$_2$D$_3$ synergistically inhibits growth of LNCaP and DU145 cells. Growth inhibition of LNCaP(**A**) and DU145(**B**) in response to LY294002 and 1,25(OH)$_2$D$_3$ alone or in combination. Cells were grown, treated and analyzed as described in Materials and Methods. Each point represents the mean and standard deviation of triplicate plates after normalization of cell number to controls (0.1% ethanol).

Figure 2. AKT inhibitors API-2 and GSK690693 synergize with 1,25(OH)$_2$D$_3$ to inhibit growth of DU145 cells and human primary prostate cancer strain. Growth inhibition of DU145 cells (**A**) and human primary prostate cancer cell strain WFU273Ca (**B**) in response to API-2 and 1,25(OH)$_2$D$_3$ alone or in combination. Growth inhibition of DU145 cells in response to GSK690693 and 1,25(OH)$_2$D$_3$ alone or in combination (**C**). Insert demonstrates PTEN and phospho-AKT levels in WFU273Ca cell strain as determined by Immunoblot. Growth inhibition of human primary prostate cancer cell strain WFU273Ca in response to GSK690693 and 1,25(OH)$_2$D$_3$ alone or in combination (**D**). Cells were grown, treated and analyzed as described in Materials and Methods.

Figure 3. AKT inhibitor API-2 and 1,25(OH)$_2$D$_3$ cooperate to induce G1-arrest in DU145 cells. DU145 cells were treated with the indicated doses for 24 hr and evaluated for cell cycle distribution as described in the Materials and Methods section. Insert demonstrates the G1/S ratios. Values are means for the triplicates ± SD. Means without a common letter are significantly different by ANOVA ($P < 0.05$).

Figure 4. AKT inhibitor API-2 and 1,25(OH)$_2$D$_3$ cooperate to induce G1 senescence and p21 levels. (A) Representative photographs of 1,25(OH)$_2$D$_3$ and API-2 inducing (SA)-β-galactosidase activity in a cooperative manner in WFU273Ca cells**. (B,C,D)** Quantitative data from multiple images of WFU273Ca cells treated as indicated. Analysis was performed as described in the Materials and Methods section**.** Means ± SE are shown. Means without a common letter are significantly different by ANOVA ($P < 0.05$). **(F)** Induction of senescence by 1,25(OH)$_2$D$_3$ alone or in presence of 0.25 μM API-2

in DU145 cells. Quantitative data from ten images of DU145 cells treated as indicated. Cells were grown, treated and (SA)-β-galactosidase activity was evaluated as described in Materials and Methods. Means ± SE are shown. Means without a common letter are significantly different by ANOVA ($P < 0.05$). **(E)** API-2 and 1,25$(OH)_2D_3$ cooperatively induce p21 and p27 protein levels in DU145 cells. DU145 cells were treated with vehicle, 0.25µM API-2 or 100 nM 1,25$(OH)_2D_3$ or the combination of the two and in 24hr protein lysates were collected and Immunoblot was carried out as described in Materials and Methods.

Figure 5. *In vitro* suppression or loss of Pten is not sufficient to antagonize 1,25$(OH)_2D_3$-mediated growth suppression. (A) Growth inhibition of WFU3 MPECs infected with Pten shRNA or scrambled shRNA in response to 1,25$(OH)_2D_3$. Values are means for the triplicates ±SD. **(B)** Pten and phospho-Akt levels of WFU3 MPEC clones infected with lentivirus expressing scrambled shRNA (control clones) or shRNA targeting Pten (Pten shRNA clones) as determined by Immunoblot. **(C)** Growth inhibition of $Pten^{lox/lox}$ and $Pten^{-/-}$ MPECs in response to 1,25$(OH)_2D_3$. $Pten^{lox/lox}$ MPECs isolated from prostates of $Pten^{lox/lox}$ Cre-recombinase negative animals and infected with lentivirus expressing self-deleting Cre-recombinase to generate $Pten^{-/-}$ MPEC. Values are means for the triplicates ±SD. **(D)** Pten and phospho-Akt levels of $Pten^{lox/lox}$ and $Pten^{-/-}$ MPECs determined by Immunoblot. Protein lysate isolated from LNCaP cells was used as controls.

Figure 6. AKT inhibitor API-2 synergizes with 1,25$(OH)_2D_3$ to inhibit growth of MPEC with reduced or lost Pten expression. Growth inhibition of Control shRNA clone 3 MPEC (**A**), Pten shRNA clone 4 (**B**) in response to API-2 and 1,25$(OH)_2D_3$ alone or in combination. MPEC were established, grown, treated and analyzed as described in Materials and Methods.

References

1. Cancer Facts and Figures.: American Cancer Society, 2007.

2. Ahonen MH, Tenkanen L, Teppo L, Hakama M, Tuohimaa P. Prostate cancer risk and prediagnostic serum 25-hydroxyvitamin D levels (Finland). Cancer Causes Control 2000;11:847-852.

3. Schwartz GG, Hulka BS. Is vitamin D deficiency a risk factor for prostate cancer? (Hypothesis). Anticancer Res 1990;10:1307-1311.

4. Banerjee P, Chatterjee M. Antiproliferative role of vitamin D and its analogs--a brief overview. Mol Cell Biochem 2003;253:247-254.

5. Rao A, Woodruff RD, Wade WN, Kute TE, Cramer SD. Genistein and vitamin D synergistically inhibit human prostatic epithelial cell growth. J Nutr 2002;132:3191-3194.

6. Peehl DM, Skowronski RJ, Leung GK, Wong ST, Stamey TA, Feldman D. Antiproliferative effects of 1,25-dihydroxyvitamin D3 on primary cultures of human prostatic cells. Cancer Res 1994;54:805-810.

7. Skowronski RJ, Peehl DM, Feldman D. Vitamin D and prostate cancer: 1,25 dihydroxyvitamin D3 receptors and actions in human prostate cancer cell lines. Endocrinology 1993;132:1952-1960.

8. Miller GJ, Stapleton GE, Hedlund TE, Moffat KA. Vitamin D receptor expression, 24-hydroxylase activity, and inhibition of growth by 1alpha,25-dihydroxyvitamin D3 in seven human prostatic carcinoma cell lines. Clin Cancer Res 1995;1:997-1003.

9. Zhao XY, Peehl DM, Navone NM, Feldman D. 1alpha,25-dihydroxyvitamin D3 inhibits prostate cancer cell growth by androgen-dependent and androgen-independent mechanisms. Endocrinology 2000;141:2548-2556.

10. Ahmed S, Johnson CS, Rueger RM, Trump DL. Calcitriol (1,25-dihydroxycholecalciferol) potentiates activity of mitoxantrone/dexamethasone in an androgen independent prostate cancer model. J Urol 2002;168:756-761.

11. Blutt SE, Weigel NL. Vitamin D and prostate cancer. Proc Soc Exp Biol Med 1999;221:89-98.

12. Getzenberg RH, Light BW, Lapco PE, Konety BR, Nangia AK, Acierno JS, Dhir R, Shurin Z, Day RS, Trump DL, Johnson CS. Vitamin D inhibition of prostate adenocarcinoma growth and metastasis in the Dunning rat prostate model system. Urology 1997;50:999-1006.

13. Krishnan AV, Peehl DM, Feldman D. Inhibition of prostate cancer growth by vitamin D: Regulation of target gene expression. J Cell Biochem 2003;88:363-371.

14. Cheng GZ, Park S, Shu S, He L, Kong W, Zhang W, Yuan Z, Wang LH, Cheng JQ. Advances of AKT pathway in human oncogenesis and as a target for anti-cancer drug discovery. Curr Cancer Drug Targets 2008;8:2-6.

15. Li DM, Sun H. PTEN/MMAC1/TEP1 suppresses the tumorigenicity and induces G1 cell cycle arrest in human glioblastoma cells. Proc Natl Acad Sci U S A 1998;95:15406-15411.

16. Li L, Ittmann MM, Ayala G, Tsai MJ, Amato RJ, Wheeler TM, Miles BJ, Kadmon D, Thompson TC. The emerging role of the PI3-K-Akt pathway in prostate cancer progression. Prostate Cancer Prostatic Dis 2005;8:108-118.

17. Rubin MA, Gerstein A, Reid K, Bostwick DG, Cheng L, Parsons R, Papadopoulos N. 10q23.3 loss of heterozygosity is higher in lymph node-positive (pT2-3,N+) versus lymph node-negative (pT2-3,N0) prostate cancer. Hum Pathol 2000;31:504-508.

18. Sansal I, Sellers WR. The biology and clinical relevance of the PTEN tumor suppressor pathway. J Clin Oncol 2004;22:2954-2963.

19. Sellers WR, Sawyers CL. Somatic genetics of prostate cancer: Oncogenes and tumor supressors. Philadelphia, PA: Lippencott, William & Wilkins, 2002.

20. Viglietto G, Motti ML, Bruni P, Melillo RM, D'Alessio A, Califano D, Vinci F, Chiappetta G, Tsichlis P, Bellacosa A, Fusco A, Santoro M. Cytoplasmic relocalization and inhibition of the cyclin-dependent kinase inhibitor p27(Kip1) by PKB/Akt-mediated phosphorylation in breast cancer. Nat Med 2002;8:1136-1144.

21. Kops GJ, de Ruiter ND, De Vries-Smits AM, Powell DR, Bos JL, Burgering BM. Direct control of the Forkhead transcription factor AFX by protein kinase B. Nature 1999;398:630-634.

22. Mamillapalli R, Gavrilova N, Mihaylova VT, Tsvetkov LM, Wu H, Zhang H, Sun H. PTEN regulates the ubiquitin-dependent degradation of the CDK inhibitor p27(KIP1) through the ubiquitin E3 ligase SCF(SKP2). Curr Biol 2001;11:263-267.

23. Andreu EJ, Lledo E, Poch E, Ivorra C, Albero MP, Martinez-Climent JA, Montiel-Duarte C, Rifon J, Perez-Calvo J, Arbona C, Prosper F, Perez-Roger I. BCR-ABL induces the expression of Skp2

through the PI3K pathway to promote p27Kip1 degradation and proliferation of chronic myelogenous leukemia cells. Cancer Res 2005;65:3264-3272.

24. Motti ML, Califano D, Troncone G, De Marco C, Migliaccio I, Palmieri E, Pezzullo L, Palombini L, Fusco A, Viglietto G. Complex regulation of the cyclin-dependent kinase inhibitor p27kip1 in thyroid cancer cells by the PI3K/AKT pathway: regulation of p27kip1 expression and localization. Am J Pathol 2005;166:737-749.

25. Barclay WW, Cramer SD. Culture of mouse prostatic epithelial cells from genetically engineered mice. Prostate 2005;63:291-298.

26. Deng Z, Wan M, Sui G. PIASy-mediated sumoylation of Yin Yang 1 depends on their interaction but not the RING finger. Mol Cell Biol 2007;27:3780-3792.

27. Barclay WW, Axanova LS, Chen W, Romero L, Maund SL, Soker S, Lees CJ, Cramer SD. Characterization of adult prostatic progenitor/stem cells exhibiting self-renewal and multilineage differentiation. Stem Cells 2008;26:600-610.

28. Lesche R, Groszer M, Gao J, Wang Y, Messing A, Sun H, Liu X, Wu H. Cre/loxP-mediated inactivation of the murine Pten tumor suppressor gene. Genesis 2002;32:148-149.

29. Berquin IM, Min Y, Wu R, Wu H, Chen YQ. Expression signature of the mouse prostate. J Biol Chem 2005;280:36442-36451.

30. Pfeifer A, Brandon EP, Kootstra N, Gage FH, Verma IM. Delivery of the Cre recombinase by a self-deleting lentiviral vector: efficient gene targeting in vivo. Proc Natl Acad Sci U S A 2001;98:11450-11455.

31. Barclay WW, Woodruff RD, Hall MC, Cramer SD. A system for studying epithelial-stromal interactions reveals distinct inductive abilities of stromal cells from benign prostatic hyperplasia and prostate cancer. Endocrinology 2005;146:13-18.

32. Peehl DM. Culture of human prostatic epithelial cells. New York: Wiley Liss, Inc, 1992.

33. Yang L, Dan HC, Sun M, Liu Q, Sun XM, Feldman RI, Hamilton AD, Polokoff M, Nicosia SV, Herlyn M, Sebti SM, Cheng JQ. Akt/protein kinase B signaling inhibitor-2, a selective small molecule inhibitor of Akt signaling with antitumor activity in cancer cells overexpressing Akt. Cancer Res 2004;64:4394-4399.

34. Dimri GP, Lee X, Basile G, Acosta M, Scott G, Roskelley C, Medrano EE, Linskens M, Rubelj I, Pereira-Smith O, et al. A biomarker that identifies senescent human cells in culture and in aging skin in vivo. Proc Natl Acad Sci U S A 1995;92:9363-9367.

35. Vlahos CJ, Matter WF, Hui KY, Brown RF. A specific inhibitor of phosphatidylinositol 3-kinase, 2-(4-morpholinyl)-8-phenyl-4H-1-benzopyran-4-one (LY294002). J Biol Chem 1994;269:5241-5248.

36. Chou TC, Talalay P. Quantitative analysis of dose-effect relationships: the combined effects of multiple drugs or enzyme inhibitors. Adv Enzyme Regul 1984;22:27-55.

37. Zhuang SH, Schwartz GG, Cameron D, Burnstein KL. Vitamin D receptor content and transcriptional activity do not fully predict antiproliferative effects of vitamin D in human prostate cancer cell lines. Mol Cell Endocrinol 1997;126:83-90.

38. Ihle NT, Powis G. Take your PIK: phosphatidylinositol 3-kinase inhibitors race through the clinic and toward cancer therapy. Mol Cancer Ther 2009;8:1-9.

39. Rhodes N, Heerding DA, Duckett DR, Eberwein DJ, Knick VB, Lansing TJ, McConnell RT, Gilmer TM, Zhang SY, Robell K, Kahana JA, Geske RS, Kleymenova EV, Choudhry AE, Lai Z, Leber JD, Minthorn EA, Strum SL, Wood ER, Huang PS, Copeland RA, Kumar R. Characterization of an Akt kinase inhibitor with potent pharmacodynamic and antitumor activity. Cancer Res 2008;68:2366-2374.

40. Berquin IM, Min Y, Wu R, Wu J, Perry D, Cline JM, Thomas MJ, Thornburg T, Kulik G, Smith A, Edwards IJ, D'Agostino R, Zhang H, Wu H, Kang JX, Chen YQ. Modulation of prostate cancer genetic risk by omega-3 and omega-6 fatty acids. J Clin Invest 2007;117:1866-1875.

41. Beer TM, Eilers KM, Garzotto M, Egorin MJ, Lowe BA, Henner WD. Weekly high-dose calcitriol and docetaxel in metastatic androgen-independent prostate cancer. J Clin Oncol 2003;21:123-128.

42. Campisi J, d'Adda di Fagagna F. Cellular senescence: when bad things happen to good cells. Nat Rev Mol Cell Biol 2007;8:729-740.

43. Michaloglou C, Vredeveld LC, Soengas MS, Denoyelle C, Kuilman T, van der Horst CM, Majoor DM, Shay JW, Mooi WJ, Peeper DS. BRAFE600-associated senescence-like cell cycle arrest of human naevi. Nature 2005;436:720-724.

44. Courtois-Cox S, Genther Williams SM, Reczek EE, Johnson BW, McGillicuddy LT, Johannessen CM, Hollstein PE, MacCollin M, Cichowski K. A negative feedback signaling network underlies oncogene-induced senescence. Cancer Cell 2006;10:459-472.

45. Schmitt CA, Fridman JS, Yang M, Lee S, Baranov E, Hoffman RM, Lowe SW. A senescence program controlled by p53 and p16INK4a contributes to the outcome of cancer therapy. Cell 2002;109:335-346.

46. Collado M, Gil J, Efeyan A, Guerra C, Schuhmacher AJ, Barradas M, Benguria A, Zaballos A, Flores JM, Barbacid M, Beach D, Serrano M. Tumour biology: senescence in premalignant tumours. Nature 2005;436:642.

47. Majumder PK, Grisanzio C, O'Connell F, Barry M, Brito JM, Xu Q, Guney I, Berger R, Herman P, Bikoff R, Fedele G, Baek WK, Wang S, Ellwood-Yen K, Wu H, Sawyers CL, Signoretti S, Hahn WC, Loda M, Sellers WR. A prostatic intraepithelial neoplasia-dependent p27 Kip1 checkpoint induces senescence and inhibits cell proliferation and cancer progression. Cancer Cell 2008;14:146-155.

48. Chen Z, Trotman LC, Shaffer D, Lin HK, Dotan ZA, Niki M, Koutcher JA, Scher HI, Ludwig T, Gerald W, Cordon-Cardo C, Pandolfi PP. Crucial role of p53-dependent cellular senescence in suppression of Pten-deficient tumorigenesis. Nature 2005;436:725-730.

49. Han XL, Wu FG, Zhang ZY, Tong TJ. Posttranscriptional induction of p21Waf1 mediated by ectopic p16INK4 in human diploid fibroblast. Chin Med J (Engl) 2007;120:405-409.

50. Vigneron A, Roninson IB, Gamelin E, Coqueret O. Src inhibits adriamycin-induced senescence and G2 checkpoint arrest by blocking the induction of p21waf1. Cancer Res 2005;65:8927-8935.

51. Alexander K, Hinds PW. Requirement for p27(KIP1) in retinoblastoma protein-mediated senescence. Mol Cell Biol 2001;21:3616-3631.

52. Yang ES, Burnstein KL. Vitamin D inhibits G1 to S progression in LNCaP prostate cancer cells through p27Kip1 stabilization and Cdk2 mislocalization to the cytoplasm. J Biol Chem 2003;278:46862-46868.

Figure 1

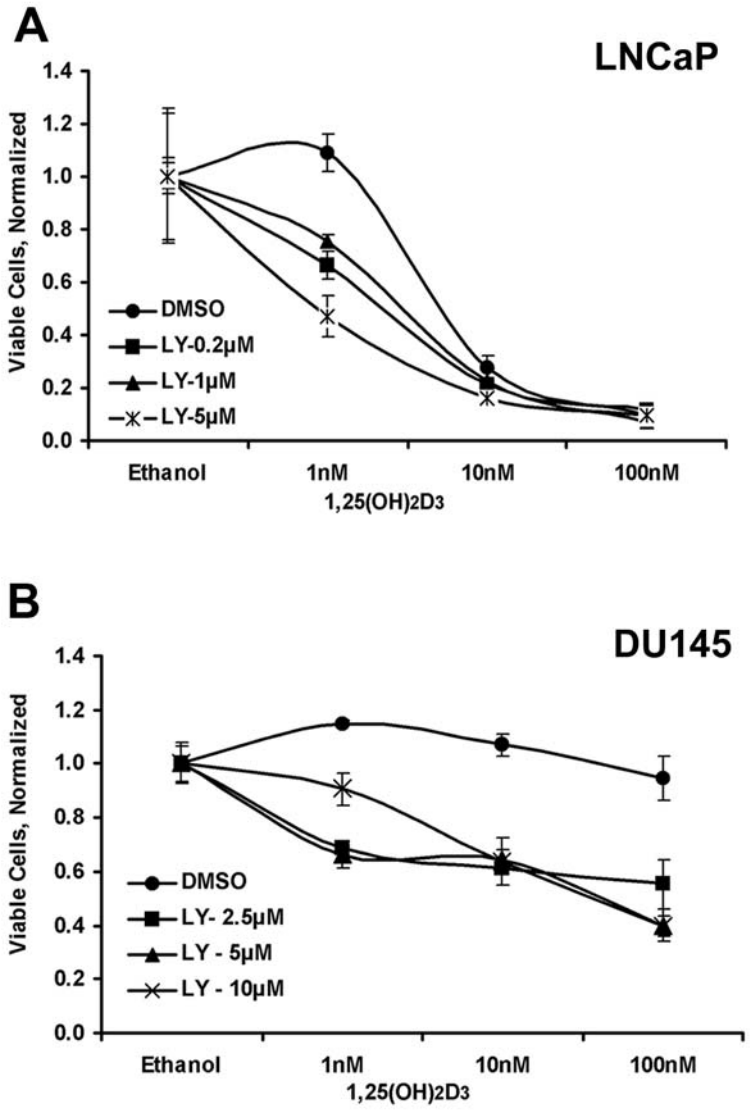
A
LNCaP
Viable Cells, Normalized
1.4
1.2
1.0
0.8
0.6
0.4
0.2
0.0
DMSO
LY-0.2μM
LY-1μM
LY-5μM
Ethanol
1nM
10nM
100nM
1,25(OH)2D3
B
DU145
Viable Cells, Normalized
1.4
1.2
1.0
0.8
0.6
0.4
0.2
0.0
DMSO
LY- 2.5μM
LY - 5μM
LY - 10μM
Ethanol
1nM
10nM
100nM
1,25(OH)2D3

Figure 2

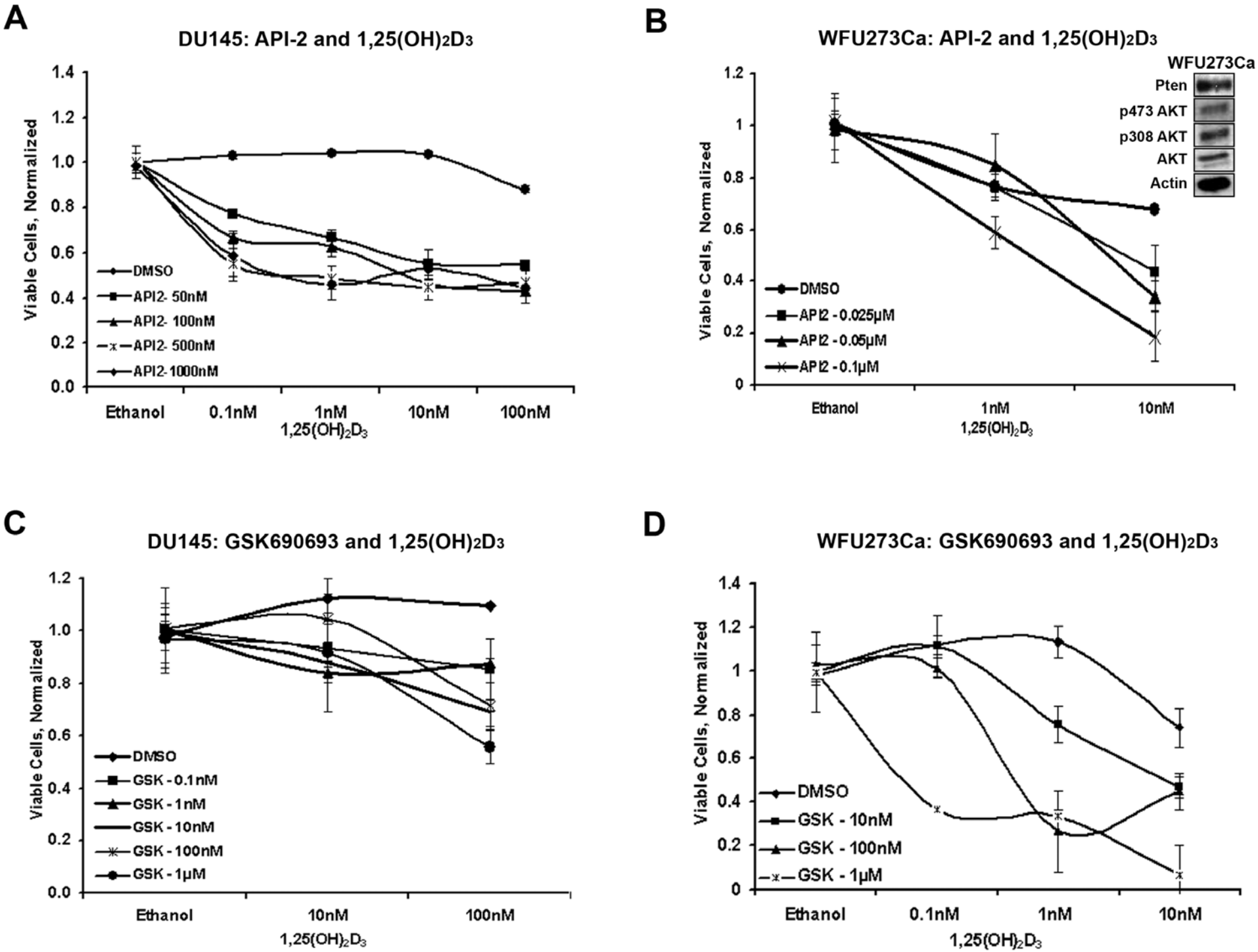
A
DU145: API-2 and 1,25(OH)2D3
Viable Cells, Normalized
1.4
1.2
1.0
0.8
0.6
0.4
0.2
0.0
DMSO
API2- 50nM
API2- 100nM
API2- 500nM
API2-1000nM
Ethanol
0.1nM
1nM
10nM
100nM
1,25(OH)2D3
B
WFU273Ca: API-2 and 1,25(OH)2D3
WFU273Ca
Pten
p473 AKT
p308 AKT
AKT
Actin
Viable Cells, Normalized
1.2
1
0.8
0.6
0.4
0.2
0
DMSO
API2 - 0.025μM
API2 - 0.05μM
API2 - 0.1μM
Ethanol
1nM
10nM
1,25(OH)2D3
C
DU145: GSK690693 and 1,25(OH)2D3
Viable Cells, Normalized
1.2
1.0
0.8
0.6
0.4
0.2
0.0
DMSO
GSK - 0.1nM
GSK - 1nM
GSK - 10nM
GSK - 100nM
GSK - 1μM
Ethanol
10nM
100nM
1,25(OH)2D3
D
WFU273Ca: GSK690693 and 1,25(OH)2D3
Viable Cells, Normalized
1.4
1.2
1
0.8
0.6
0.4
0.2
0
DMSO
GSK - 10nM
GSK - 100nM
GSK - 1μM
Ethanol
0.1nM
1nM
10nM
1,25(OH)2D3

Figure 3

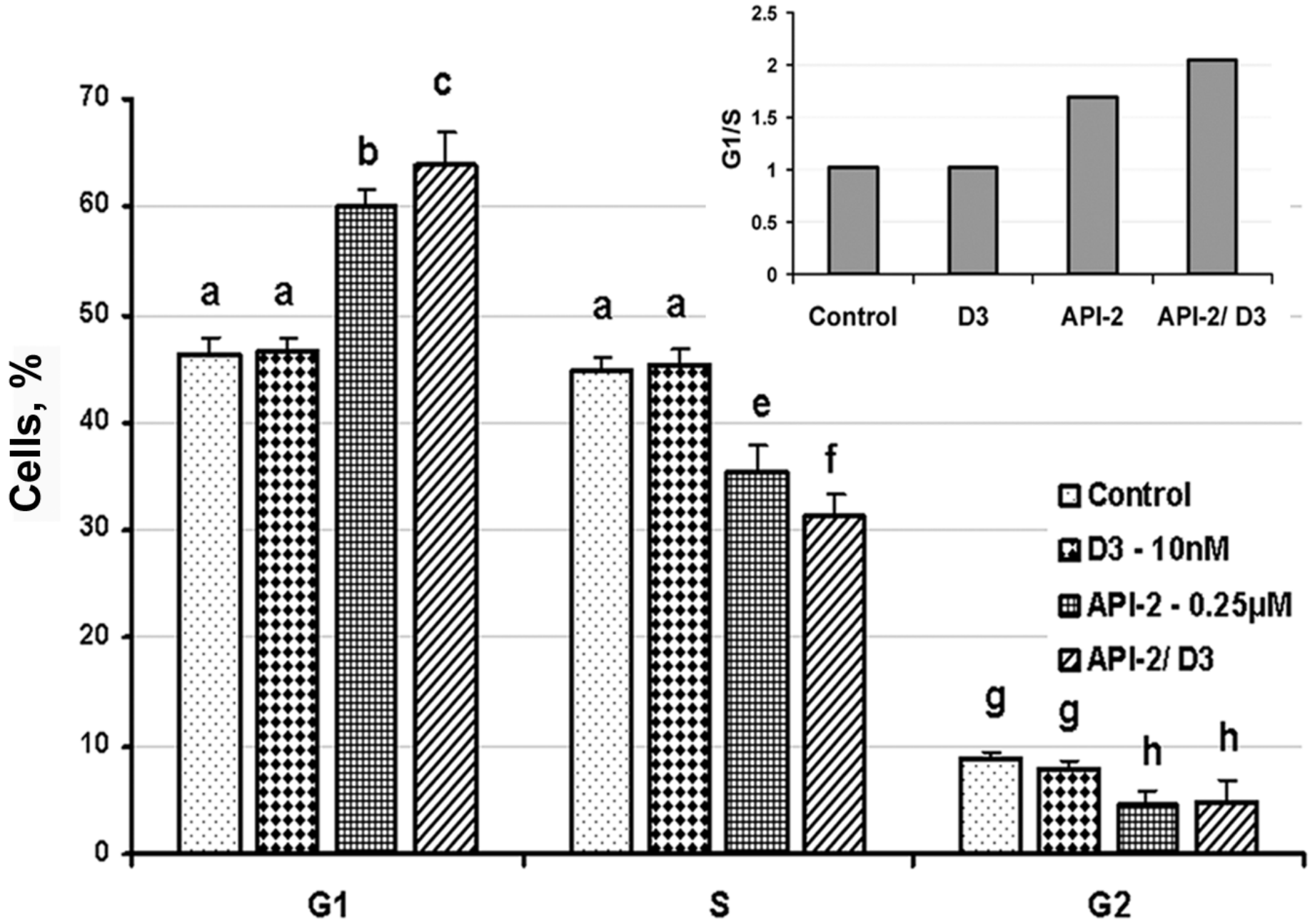
Cells, %
70
60
50
40
30
20
10
0
a
a
b
c
a
a
e
f
g
g
h
h
G1
S
G2
Control
D3 - 10nM
API-2 - 0.25μM
API-2/ D3
G1/S
2.5
2
1.5
1
0.5
0
Control
D3
API-2
API-2/ D3

Figure 4

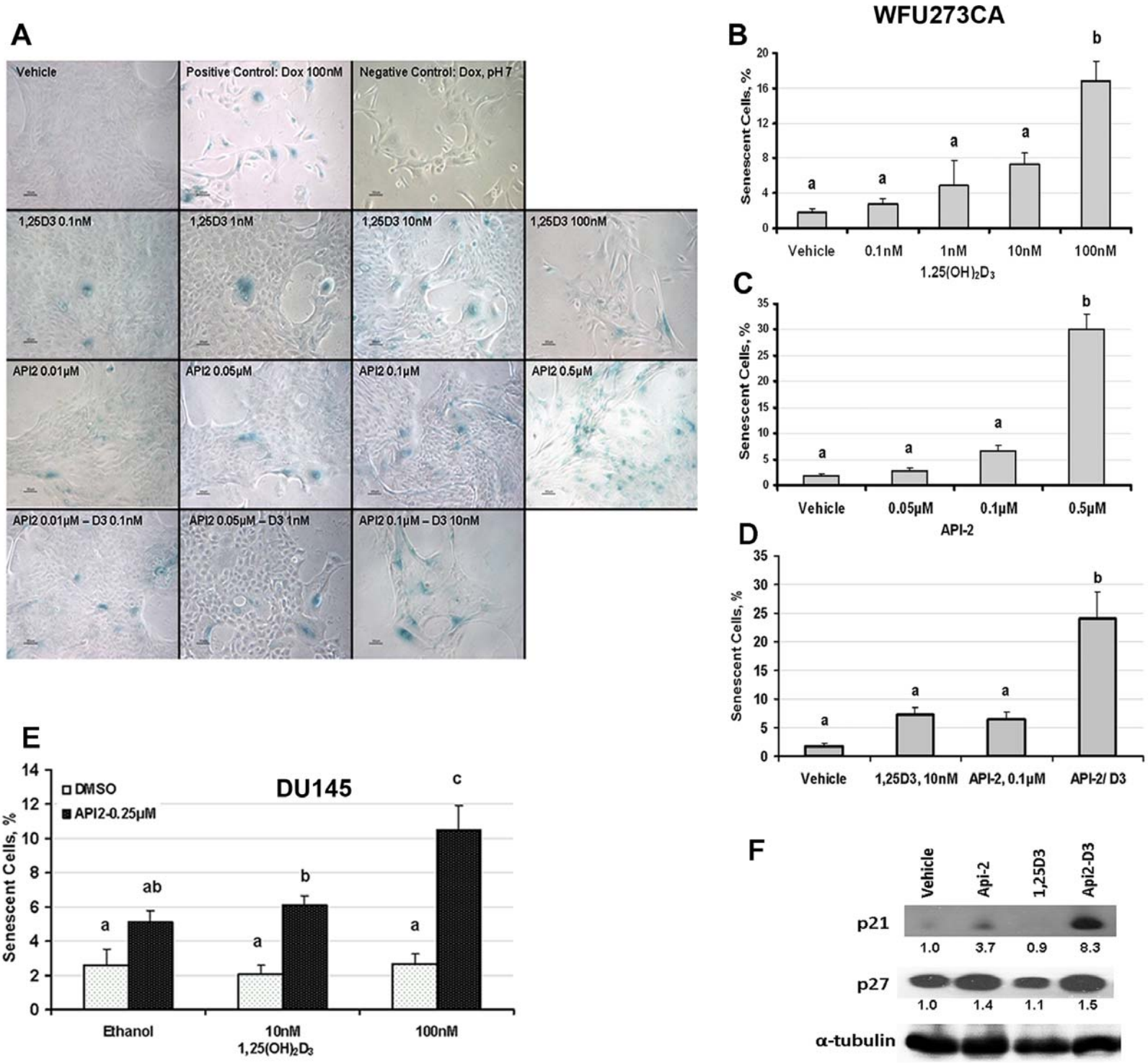
A
Vehicle
Positive Control: Dox 100nM
Negative Control: Dox, pH 7
1,25D3 0.1nM
1,25D3 1nM
1,25D3 10nM
1,25D3 100nM
API2 0.01μM
API2 0.05μM
API2 0.1μM
API2 0.5μM
API2 0.01μM – D3 0.1nM
API2 0.05μM – D3 1nM
API2 0.1μM – D3 10nM
WFU273CA
B
Senescent Cells, %
Vehicle
0.1nM
1nM
10nM
100nM
1.25(OH)2D3
C
Senescent Cells, %
Vehicle
0.05μM
0.1μM
0.5μM
API-2
D
Senescent Cells, %
Vehicle
1,25D3, 10nM
API-2, 0.1μM
API-2/ D3
E
DU145
DMSO
API2-0.25μM
Senescent Cells, %
Ethanol
10nM
100nM
1,25(OH)2D3
F
Vehicle
Api-2
1,25D3
Api2-D3
p21
1.0
3.7
0.9
8.3
p27
1.0
1.4
1.1
1.5
α-tubulin

Figure 5

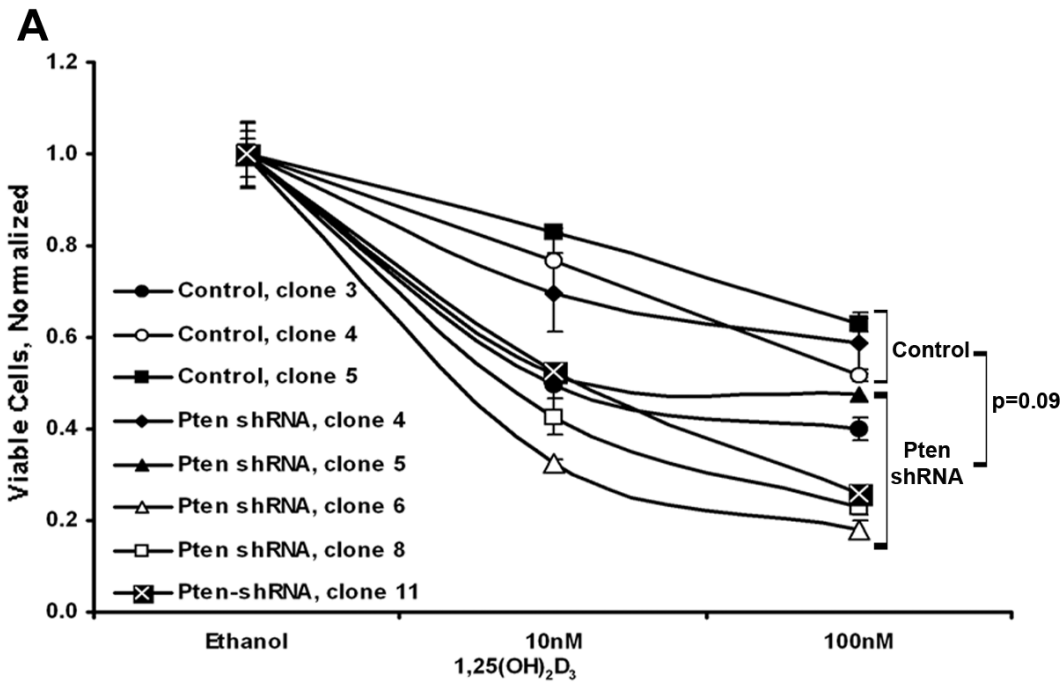
A
Viable Cells, Normalized
1.2
1.0
0.8
0.6
0.4
0.2
0.0
Control, clone 3
Control, clone 4
Control, clone 5
Pten shRNA, clone 4
Pten shRNA, clone 5
Pten shRNA, clone 6
Pten shRNA, clone 8
Pten-shRNA, clone 11
Control
Pten shRNA
p=0.09
Ethanol
10nM
100nM
1,25(OH)2D3

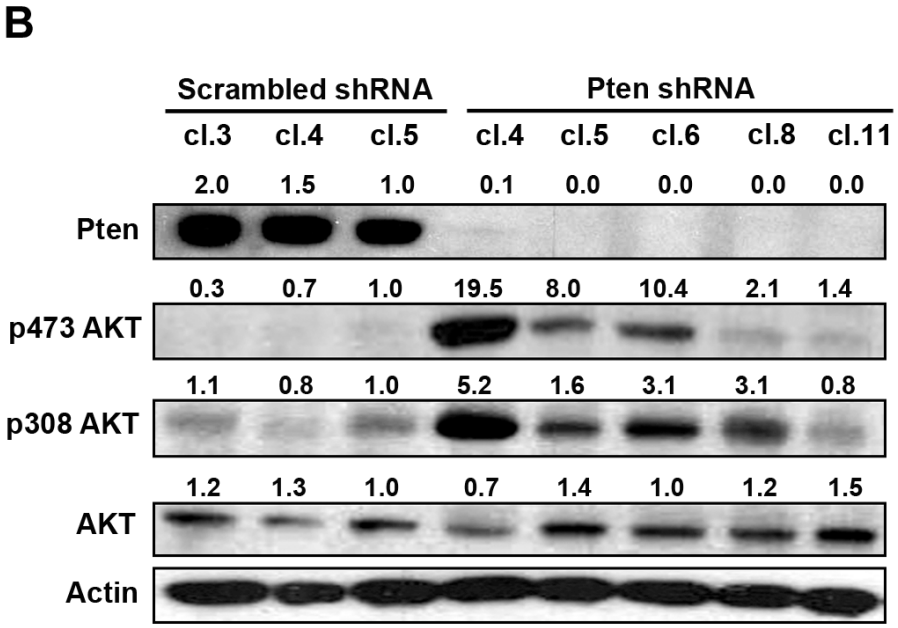
B
Scrambled shRNA
Pten shRNA
cl.3 cl.4 cl.5 cl.4 cl.5 cl.6 cl.8 cl.11
2.0 1.5 1.0 0.1 0.0 0.0 0.0 0.0
Pten
0.3 0.7 1.0 19.5 8.0 10.4 2.1 1.4
p473 AKT
1.1 0.8 1.0 5.2 1.6 3.1 3.1 0.8
p308 AKT
1.2 1.3 1.0 0.7 1.4 1.0 1.2 1.5
AKT
Actin

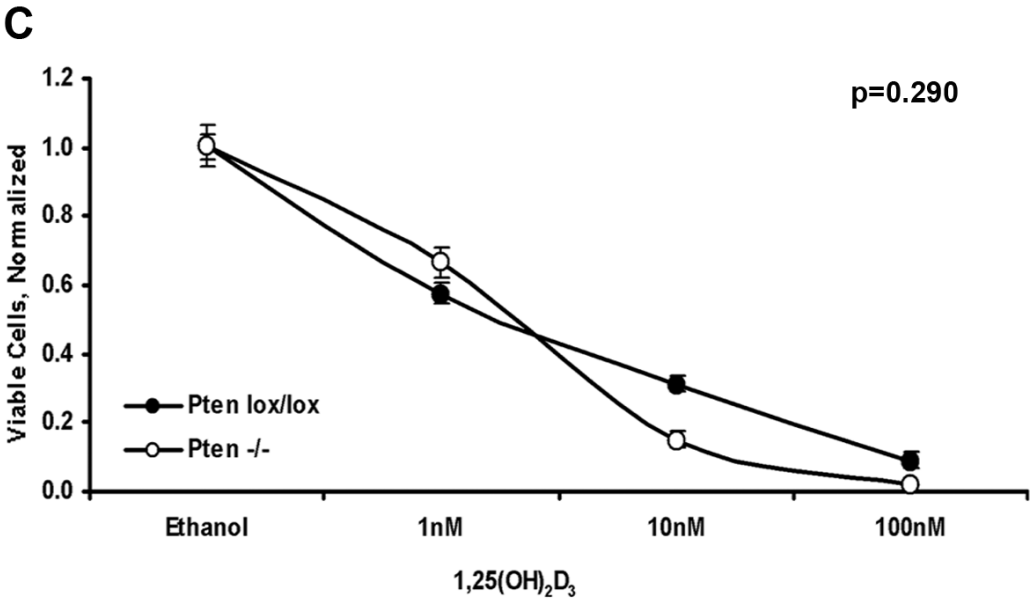
C
p=0.290
Viable Cells, Normalized
1.2
1.0
0.8
0.6
0.4
0.2
0.0
Pten lox/lox
Pten -/-
Ethanol
1nM
10nM
100nM
1,25(OH)2D3

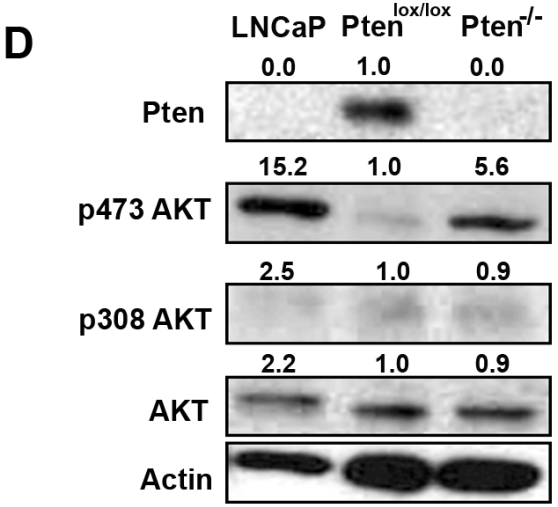
D
LNCaP Pten lox/lox Pten -/-
0.0 1.0 0.0
Pten
15.2 1.0 5.6
p473 AKT
2.5 1.0 0.9
p308 AKT
2.2 1.0 0.9
AKT
Actin

Figure 6

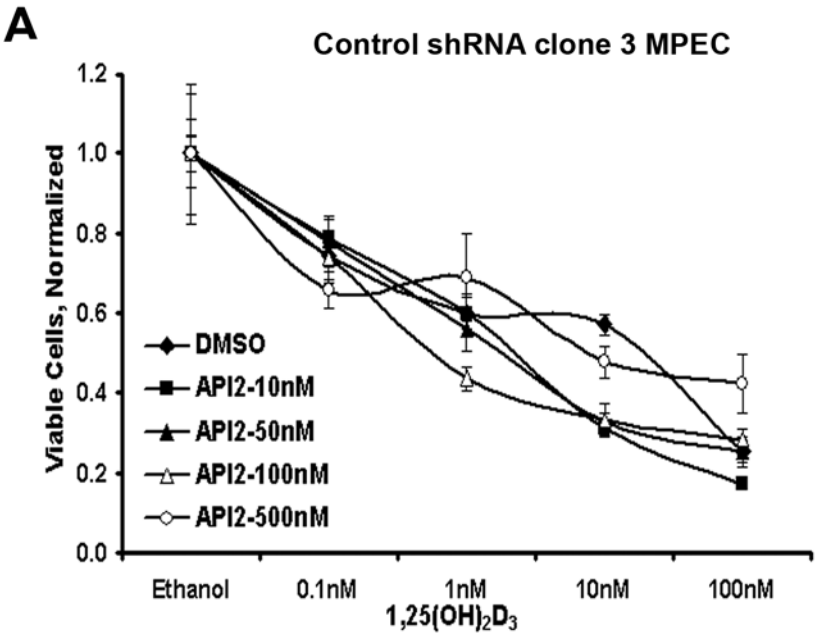
A
Control shRNA clone 3 MPEC
Viable Cells, Normalized
1.2
1.0
0.8
0.6
0.4
0.2
0.0
DMSO
API2-10nM
API2-50nM
API2-100nM
API2-500nM
Ethanol
0.1nM
1nM
10nM
100nM
1,25(OH)2D3

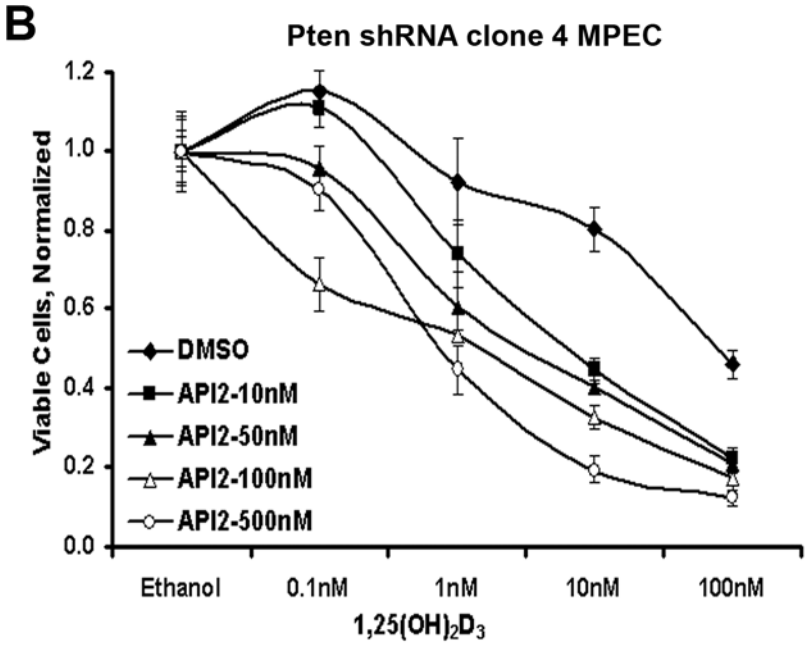
B
Pten shRNA clone 4 MPEC
Viable Cells, Normalized
1.2
1.0
0.8
0.6
0.4
0.2
0.0
DMSO
API2-10nM
API2-50nM
API2-100nM
API2-500nM
Ethanol
0.1nM
1nM
10nM
100nM
1,25(OH)2D3

Table I. Synergism between 1,25(OH)$_2$D$_3$ and LY294002 in LNCaP and DU145 cells***

	1,25(OH)2D3, nM	LY294002, µM	CI*	DRI**		Synergism
				1,25(OH)$_2$D$_3$	LY294002	
LNCaP						
	1	**0.2**	**0.171**	**8.2**	**20.7**	**Strong**
	1	**1**	**0.298**	**10.9**	**4.8**	**Strong**
	1	**0.5**	**0.675**	**26.3**	**1.6**	**Moderate**
DU145						
	1	**2.5**	**0.408**	**513.8**	**2.5**	**Intermediate**
	1	**5**	**0.650**	**666.0**	**1.5**	**Intermediate**
	10	**2.5**	**0.382**	**58.2**	**2.8**	**Intermediate**
	10	**5**	**0.654**	**67.7**	**1.6**	**Intermediate**
	10	**10**	**0.801**	**117.6**	**1.3**	**Moderate**
	100	**2.5**	**0.489**	**6.4**	**3.0**	**Intermediate**
	100	**5**	**0.585**	**9.5**	**2.1**	**Intermediate**
	100	**10**	**0.701**	**14.9**	**1.6**	**Intermediate**

*Combination Index (CI<0.1 indicates Very Strong Synergism; 0.1÷0.3 Strong Synergism; 0.3÷0.7 Synergism; 0.70÷0.85 Moderate Synergism; 0.85÷0.90 Slight Synergism; 0.90÷1.10 Nearly Additive Synergism).

**Dose-reduction Index. DRI is calculated using the equation: $(DRI)_1=(D_x)_1/D_1$ and $(DRI)_2=(D_x)_2/D_2$, where $(D)_1$ and $(D)_2$ are the doses of drug that have *x* effect when used in combination and $(D_x)_1$ and $(D_x)_2$ are the doses of drug 1 and drug 2 that have the same *x* effect when used alone.

*** Data are from assays depicted in Figure 1, only statistically significantly different means by ANOVA are depicted.

Table II. Synergism between $1,25(OH)_2D_3$ and AKT Inhibitors***

1,25(OH)2D3, nM	AKT inhibitor, nM	CI*	DRI**		Synergism
			$1,25(OH)_2D_3$	AKT Inhibitor	
DU145					
AKT Inhibitor: API-2					
0.1	50	$0.18*10^{-6}$	$5.5*10^{4}$	$4.0*10^{6}$	Very Strong
0.1	100	$0.12*10^{-6}$	$8.7*10^{4}$	$4.4*10^{6}$	Very Strong
0.1	500	$7.98*10^{-6}$	$1.3*10^{5}$	$1.9*10^{6}$	Very Strong
0.1	1000	$9.82*10^{-6}$	$1.2*10^{5}$	$7.4*10^{5}$	Very Strong
1	50	$0.75*10^{-6}$	$1.3*10^{4}$	$1.8*10^{7}$	Very Strong
1	100	$0.55*10^{-6}$	$1.8*10^{4}$	$1.6*10^{7}$	Very Strong
1	500	$0.60*10^{-6}$	$1.7*10^{4}$	$2.7*10^{6}$	Very Strong
1	1000	$0.54*10^{-6}$	$1.9*10^{4}$	$1.6*10^{6}$	Very Strong
10	50	0.001	872,1	$8.8*10^{6}$	Very Strong
10	100	0.001	1014.8	$5.7*10^{6}$	Very Strong
10	500	0.001	1950.4	$3.5*10^{6}$	Very Strong
10	1000	0.001	1461.5	$1.1*10^{6}$	Very Strong
100	50	0.007	135.6	$1.9*10^{7}$	Very Strong
100	100	0.005	206.7	$1.9*10^{7}$	Very Strong
100	500	0.006	180.3	$3.1*10^{6}$	Very Strong
100	1000	0.005	193.0	$1.7*10^{6}$	Very Strong
WFU275CA					
AKT inhibitor: API-2					
0.1	0.1	0.799	283.0	1.3	Moderate
1	0.05	0.720	12.2	1.6	Moderate
1	0.1	0.714	36.9	1.5	Moderate
10	0.025	0.216	9.0	9.6	Strong
10	0.05	0.169	22.5	8.0	Strong
10	0.1	0.176	52.0	6.4	Strong
DU145					
AKT inhibitor: GSK690693					
10	1	0.003	$1.1*10^{6}$	391.3	Very Strong
10	10	0.070	$6.5*10^{4}$	14.3	Very Strong
100	0.1	0.0001	$2.3*10^{4}$	2241.4	Very Strong
100	1	0.004	$3.9*10^{4}$	268.7	Very Strong
100	10	0.010	$1.5*10^{6}$	96.9	Very Strong
100	100	0.061	$6.6*10^{6}$	16.3	Very Strong
100	1000	0.281	$6.0*10^{7}$	3.5	Strong
WFU273CA					
AKT inhibitor: GSK690693					
0.1	1000	0.773	5158.7	1.3	Moderate
1	10	0.062	37.1	28.5	Very Strong
1	100	0.120	255.9	8.7	Strong
1	1000	0.747	550.1	1.3	Moderate
10	10	0.115	10.5	51.7	Strong
10	100	0.234	14.1	6.1	Strong
10	1000	0.344	215.4	3.0	Intermediate

*Combination Index (CI<0.1 indicates Very Strong Synergism; 0.1÷0.3 Strong Synergism; 0.3÷0.7 Synergism; 0.70÷0.85 Moderate Synergism; 0.85÷0.90 Slight Synergism; 0.90÷1.10 Nearly Additive Synergism)

**Dose-reduction Index. DRI is calculated using the equation: $(DRI)_1=(D_x)_1/D_1$ and $(DRI)_2=(D_x)_2/D_2$, where $(D)_1$ and $(D)_2$ are the doses of drug that have *x* effect when used in combination and $(D_x)_1$ and $(D_x)_2$ are the doses of drug 1 and drug 2 that have the same *x* effect when used alone. DRI values for $1,25(OH)_2D_3$ treatment in DU145 are high due to inability of the program to correctly calculate DRI based on the formula as the x effect of the $1,25(OH)_2D_3$ alone is near zero.

*** Data are from assays depicted in Figure 2, only statistically significantly different means by ANOVA are depicted.

Table III. Synergism between 1,25(OH)$_2$D$_3$ and API-2 in MPEC***

1,25(OH)2D3, nM	LY294002, µM	CI*	DRI**		Synergism
			1,25(OH)$_2$D$_3$	API-2	
Control shRNA cl. 3 MPEC					
10	50	0.370	4.7	6.3	Intermediate
10	100	0.334	13.8	5.5	Intermediate
Pten shRNA cl. 4 MPEC					
0.1	500	0.018	57.2	9354.0	Very Strong
1	50	0.112	8.9	4121.8	Strong
1	100	0.099	10.1	2257.8	Very Strong
1	500	0.013	81.9	2122.8	Very Strong
10	10	0.217	4.6	$6.9*10^4$	Strong
10	50	0.134	7.5	$2.0*10^4$	Strong
10	100	0.095	10.5	$1.3*10^4$	Very Strong
10	500	0.013	78.8	$1.1*10^4$	Very Strong
100	10	0.246	4.1	$3.5*10^5$	Strong
100	50	0.205	4.9	$8.0*10^4$	Strong
100	100	0.177	5.6	$4.4*10^4$	Strong
100	500	0.048	20.7	$2.3*10^4$	Very Strong

*Combination Index (CI<0.1 indicates Very Strong Synergism; 0.1÷0.3 Strong Synergism; 0.3÷0.7 Synergism; 0.70÷0.85 Moderate Synergism; 0.85÷0.90 Slight Synergism; 0.90÷1.10 Nearly Additive Synergism)

**Dose-response Index. DRI is calculated using the equation: $(DRI)_1=(D_x)_1/D_1$ and $(DRI)_2=(D_x)_2/D_2$, where $(D)_1$ and $(D)_2$ are the doses of drug that have *x* effect when used in combination and $(D_x)_1$ and $(D_x)_2$ are the doses of drug 1 and drug 2 that have the same *x* effect when used alone.

*** Data are from assays depicted in Figure 6, only statistically significantly different means by ANOVA are depicted.